공학박사학위논문

Rheological properties and microstructural analysis of bimodal suspensions with highly size-asymmetric particles

이분산현탁액의 유변학적 성질과 미세구조 해석

2016 년 2 월

서울대학교 대학원

화학생물공학부

이 주 영

Abstract

Rheological properties and microstructural analysis of bimodal suspensions with highly size-asymmetric particles

Lee, Jooyoung
School of Chemical and Biological Engineering
The Graduate School
Seoul National University

Coating fluids that include highly size-asymmetric particles are widely used in many applications such as Li-ion batteries, multi-layer ceramic capacitors, and electrical conductors. They include different types of particles to improve the performance of the product. In these liquids, the size of the particles is very different; one is micrometer and the other nanometer scale, for example. Because of distinctively different size of the particles, these bimodal dispersions show more complex flow behavior compared to colloids of a single size. However, most studies for bi-modal dispersions assumed well-stabilized nanoparticles, thus they have not been relevant to the behavior of the materials used in industry.

In this study, a model system consisting of two kinds of particles with

highly asymmetric size was designed to offer a valuable description of complex behavior of the slurries, using a suspension consisting of polystyrene latex (500 nm) and alumina-coated silica (12 nm) particles. The surface potential of small particles was tuned by varying the solution pH, causing them to be repulsive to each other, attractive to each other, and oppositely charged to the large particles, while the large particles remained electrostatically stabilized.

The effect of addition of small particles on the rheological properties of bimodal suspensions was investigated in terms of surface chemistry and concentration of small particles. The rheological properties were dramatically changed from viscous to gel-like depending on the surface potential and concentration of small particles. A colloidal gel was induced by small particles when the small particles had the opposite charge to the large particles and a volume fraction of $10^{-4} < \phi_{small} < 10^{-3}$, and when the small particles were attractive to each other above a critical threshold, $\phi_{small} > 10^{-4}$. Cryo-SEM distinguished the gel structures to be either short bridging gels produced by oppositely charged small particles, or long bridging gels or dense gels produced by attractive small particles. On the basis of this rheological behavior and microstructure, a phase diagram of highly size-asymmetric bimodal colloids was presented with respect to the

surface chemistry and concentration of small particles.

When the mutually attractive small particles are added to suspension of highly charged large particles, a new type of colloidal gel was induced which is not described by the typical power - law scaling for fractal clusters. Their elastic moduli have a unique scaling behavior on particle volume fraction with two distinct power - law indices. The unique scaling behavior arises from the non-fractal networks of large particles that are bridged by small particle clusters in the region between the lower and the upper critical boundary of small particle volume fraction.

Because the model fluid in this study is similar to the slurries used in industry with respect to the size ratio, the range of concentration, and the surface potential, it is expected that the slurries encountered in practice have analogous mechanical behavior and microstructure to this model fluid. This study consequently provides a guideline for the design of such complex fluids and understanding of their complex flow behavior.

Keywords: Bimodal suspension, highly size-asymmetric particles, scaling behavior, microstructure, dispersion stability
Student Number: 2010-30252

Contents

List of Figures

List of tables

Chapter 1. Introduction

1.1. Coating material: bimodal suspension

Coating fluids which contain highly size-asymmetric particles are widely used in many applications, including Li-ion batteries, multi-layer ceramic capacitors, and electrical conductors [1-8]. To obtain a desired performance in the final product, particles of different size and surface potential are often used together, which can bring about unexpected results such as aggregation of particles and changing rheological behavior.

These types of complex behavior have been investigated in various model systems of highly size-asymmetric particles, and can be classified based on the relationships of surface potentials between large and small particles. When the two particles are large and small hard spheres, the depletion effect arises because of the size mismatch between the constituent particles, resulting in an attractive interaction between the large particles [9-14]. In a model system of positively and negatively charged particles, the attractive interaction between the small and large particles induces bridging between two or more large particles to form bigger aggregates [15-19]. The large particles, which are negligibly charged, are stabilized by the addition of well stabilized small particles [20-24]. However, the systems used in the previous studies used well-stabilized nanoparticles, which are quite different

from the materials used in industry.

Slurries used in industry include polymers to induce interparticle repulsion and colloidal stability. The polymers adsorb onto the surface of the particles, and are used because the particles are typically suspended in organic solvent, where stabilization by electrostatic double layer is not effective. Unfortunately, polymers do not thoroughly adsorb onto small particles with sizes of a few nanometers. Consequently, under this condition the nanoparticles are not well dispersed or have various surface potential, while large particles are stabilized and have uniform surface potential. To understand the behavior of binary particle systems used in industry, therefore, it is need to devise a new type of model system composed of various surface potential levels of nanoparticles.

In this thesis, a model system consisting of two different kinds of particles with highly asymmetric sizes was designed, using polystyrene latex (500 nm) and alumina-coated silica (12 nm). The surface potential of the small particles was tuned by adjusting the solution pH, and the various pH selectively made the small particles repulsive to each other, attractive to each other, and oppositely charged to the large particles. The large particles remained electrostatically stabilized despite the varying pH. This thesis is confined to the systems in which large particles are stable, which is typical

in industrial applications. In first part, a systematic study has been performed to understand the effect of surface potential of nano particles on the complex behavior of bimodal suspensions. The microstructure and rheological behavior of the bimodal slurries was analyzed based on the concentration and surface potential of the small particles. The addition of small particles into the suspension of well-dispersed large particles produced a dramatic change in rheological properties, from viscous to gel, which was investigated through rheometry. The morphology of the gel phase was classified and the phase diagram of the bimodal suspension was provided with respect to the surface chemistry and concentration of small particles. The origin of particle networks is investigated by comparing the surface potentials between the constituent particles using DLVO theory.

In second part, to understand the effect of attractive nanoparticles on the behavior of bimodal suspension, surface potentials of nanoparticles was fixed which caused small particles to be attractive to each other, while the large particles to be electrostatically stabilized. The gel was induced by a very small increase in the amount of attractive nano particles. The bimodal gels that formed under this condition showed behavior quite different from typical colloidal gels: the elastic moduli cannot be described by a simple power - law scaling but rather have two regions of vastly different

exponents. The existence of gels was reported to have two regions of distinct morphological characteristics, from which it is concluded that the network structure formed by the small particle clusters determines the rheological behavior of the whole bimodal gel system.

1.2. Outline of the thesis

This thesis is organized into background, experimental methods and several results on the effect of nanoparticles on the suspension of stable large particles.

The background of the research is described in Chapter 2 by dividing into importance of particle size variation in common colloidal system, overview of bimodal suspensions both in previous studies and industrial process, and scaling behavior and microstructure of typical colloidal gels. The first part of Chapter 2 describes the importance of particles size variation on the physical properties of colloidal suspension to understand the complex behavior of highly size-asymmetric particles. The second part of Chapter 2 describes the overview of bimodal suspensions both in industrial process and in previous studies, which is categorized with relation of surface potential between large and small particles. The third part introduces the scaling behavior of typical colloidal gels which is used to analyze the bimodal gels in Chapter 4.

Chapter 3 describes the properties of PS and alumina coated silica particles, experimental methods on suspension rheology and microstructure. Several methods such as cryo-SEM and small angle X-ray scattering

(SAXS) were used to analyze the microstructure of large and small particles.

In Chapter 4, the main results on the effect of nanoparticles on the suspension of stable large particles are described. In Chapter 4.1, surface properties of PS/alumina coated suspension are characterized. The suspension stability of PS suspension is confirmed in this section. Chapter 4.2 describes the results on the effect of surface chemistry of nanoparticles, with rheoloigical behavior of the suspension at various pH. A colloidal gel was induced by small particles when the small particles had the opposite charge to the large particles and a volume fraction of $10^{-4} < \phi_{small} < 10^{-3}$, and when the small particles were attractive to each other above a critical threshold, $\phi_{small} > 10^{-4}$. Microstructure of gels was investigated with cryo-SEM image in Chapter 4.2.2. The origin of this gelation is discussed with DLVO theory in Chapter 4.2.3. Finally, on the basis of microstructure and rheological behavior, phase diagram of bimodal suspension with respect to surface potential and concentration of small particles is presented in Chapter 4.2.4.

In Chapter 4.3, effect of attractive small particles on the suspension of stable large particles is focused. When the mutually attractive small particles are added to suspension of highly charged large particles, a new type of colloidal gel was induced. Chapter 4.3.1 describes the onset of gelation with

increasing the particle concentration. Chapter 4.3.2 describes their gelation behavior, which is not described by the typical power law scaling for fractal clusters. Their elastic moduli have a unique scaling behavior on particle volume fraction with two distinct power - law indices. Microstructure is observed and discussed to investigate the origin of the unique scaling behavior in Chapter 4.3.3. The non-fractal networks of large particles arise that are bridged by small particle clusters in the region between the lower and the upper critical boundary of small particle volume fraction.

Chapter 5 summarizes the main results on the works and finally suggests the several subjects that need to be considered for future works.

Chapter 2. Background

2.1. The importance of particle size variation in colloidal suspension

Colloidal suspension generally refers to a two-component system consisting of dispersed phase and the suspending medium in which characteristic length scale of dispersed phase ranges from 1 nm to 1000 nm. The elements of dispersed phase are substantially large than the molecules of surrounding medium, but they are still too small to be easily observed by the optical microscope and their motion is affected by thermal forces. Several terminology have been using in colloidal systems. For examples, when the solid particles are dispersed in the gas, they are known as aerosols. When the suspending medium is liquid, they are called as foam, emulsion, and suspension where the dispersed phase is gas, liquid and solid, respectively. Suspension, in which solid particles are dispersed in the liquid, is widely used as a coating material in the industrial applications. To improve the quality of coating products, it is important to control their complex behavior such as shear thinning, yielding, and thixotropy.

For the colloidal-sized particles, surface properties are very important because the characteristic feature of colloidal suspension is the large surface area (area to volume ratio) for the particles involved. Values for the

colloidal size range are given in Table 2.1. A typical surface area for a particle with a density of 1000 kg/m^3 and a radius of 10 nm is 300 m^2/g. Because the colloidal sized particles have such a large surface area, surface properties such as van der Waals interactions, electric double layer effects, and depletion effects play a very important role in determining the stability and physical properties of the system as a whole.

Because the particle size is closely related to the characteristic stress which results from the Brownian motion for the colloidal size range, the particle size is important factor affecting the physical properties of suspension. As given in Table 2.1, Brownian force is typically scaled on the thermal energy per characteristic volume of particles, $\sim kT/a^3$. As the particle size decreases, therefore, the characteristic stress increases in proportion to the cube of particle size, resulting in the large increase of the bulk physical properties such as viscosity and elastic modulus.

Table 2.1. Specific surface area and characteristic stress for spherical particles of a density of 1000 kg/m^3

Radius (m)	Specific surface area (m^2g^{-1})	Characteristic stress* (Pa)
10^{-9}	3×10^{3}	4.1×10^{6}
10^{-8}	3×10^{2}	4.1×10^{3}
10^{-7}	3×10^{1}	4.1×10^{0}
10^{-6}	3×10^{0}	4.1×10^{-3}

*Characteristic stress by Brownian force ~ kT/a^3

2.2. Bimodal suspension in industrial coating process

To obtain a desired performance in the final product, different types of particles with high size-asymmetry are often used together in many applications, such as the fabrication of Li-ion batteries [25, 26], multi-layer ceramic capacitors [27], electrical conductor [28], paper [29], and paints [30, 31]. The typical composition of these fluids is given in Table 2.2. In these fluids, the ratio of particle diameters between small and large particles ($q = d_{small} / d_{large}$) is typically small, often less than 0.1 [25, 26]. Such high size-asymmetry induces many unexpected problems during processing.

One of the main reasons that high size-asymmetry induces unexpected problems is that smaller particles play a much larger role in the physical properties of suspension than the large particles. As in Table 2.1, characteristic stress of 10 nm-sized particles is 106 times larger than the 1000 nm-sized particles. Therefore, nanoparticles can dominate the bulk suspension behavior, although the industrial slurries contains very small amount of nanoparticles.

High size-asymmetry induces another unexpected problem during processing because it results in an asymmetry in the surface chemistry as well as in the particle sizes. Micro-particles can be well dispersed because it

is easy to break up large aggregates and to adsorb stabilizing surfactants onto the particles. However, it is challenging to adsorb polymers thoroughly onto the particles having sizes of a few nanometers. Although much higher energy is required to breakup nanoparticles than micro-particles, slurry preparation process in most industry apply just the same energy on the whole suspension. The nanoparticles are consequently not well dispersed and have various levels of surface potentials.

Such an aggregated nanoparticle can hinder the product performance as well as induce the complex fluid behavior. There is a report on the role of nanosized particles in the function of battery products [1], where battery made by the same composition of slurry have different capacity. They changed solution pH and observed the microstructure of drying film, as in Figure 2.1(a). A sample with pH 9 shows aggregated carbon black, while pH 12 shows relatively uniform distribution of carbon black. Uniform distribution of carbon black induces to increase the capacity of battery, as in Figure 2.1(c).

Lee et al. have investigated the relation between capacity and microstructure of carbon black [2]. In that work, the same composition of cathode slurries were prepared with two different mixing sequences. Although they have the same composition, the microstructure and final

performance of batteries made by each slurries are different. Slurry of one step process which shows lower capacity has non-uniform structure of film than slurry of multi-step process. Only the distribution of carbon black was observed from EDS mapping. Lighter dots come from carbon black in Figure 2.3. Distribution of carbon black is also non-homogeneous in case of non-uniform film. From this result, it is confirmed that microstructure of carbon black is a key factor determining the film uniformity and this can be related to the performance of battery product directly. Rheological approach was taken to analyze the microstructure of these two slurries. Slurry of one-step process which has non-uniform microstructure of film and low capacity of battery shows gel-like behavior, which means that G' is higher than G'' and the modulus are independent to frequency, as shown in Figure2.4. On the other hand, in case of Slurry of multi-step process which has uniform microstructure, G' of slurry is lower than G'' and it shows liquid-like behavior. From previous studies of industrial materials, it is concluded that understanding the microstructure and rheology of bimodal suspensions is important to improve the performance of the products

(a) (b)

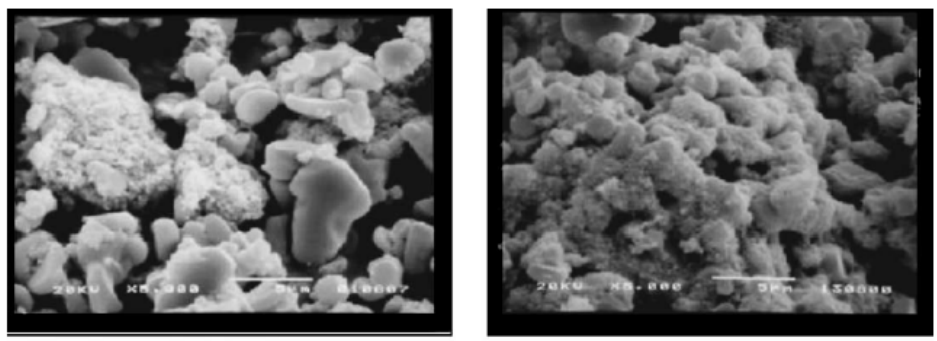

(c)

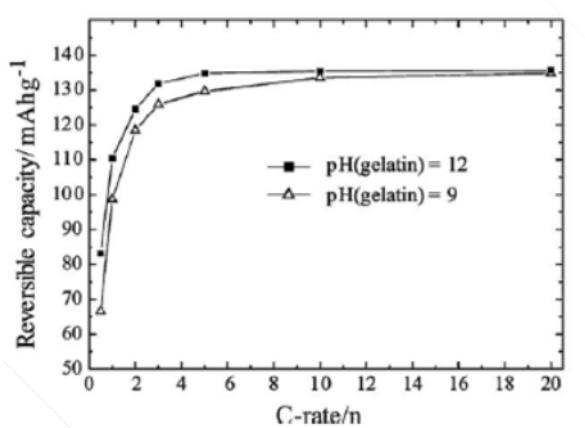

Figure 2.1. Distribution of carbon black among LiCoO2 in the case when gelatin solution had a pH of (a) 9 and (b) 12 [1]. (c) Reversible capacity as a function of C-rate for cathode materials under (a) and (b).

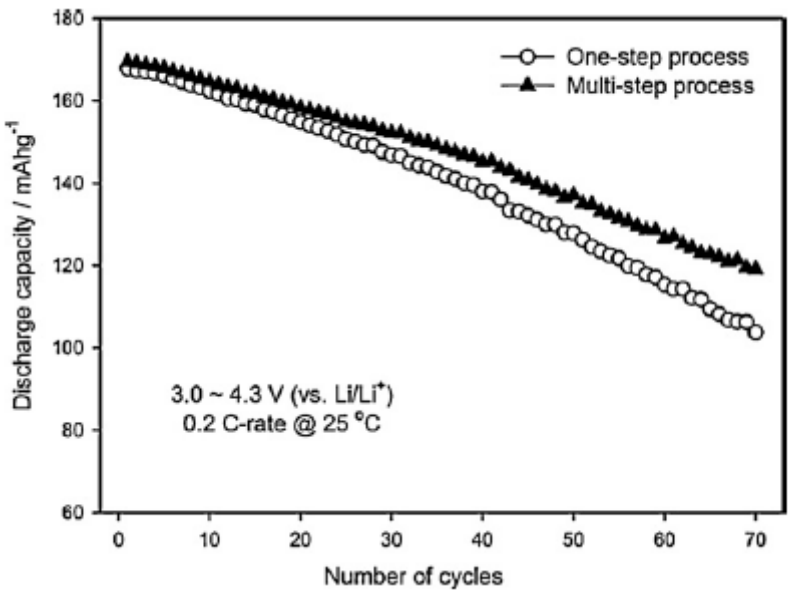

Figure 2.2. Discharge capacity observed with the Li/LiCoO2 cells according to the cycle numbe [2].

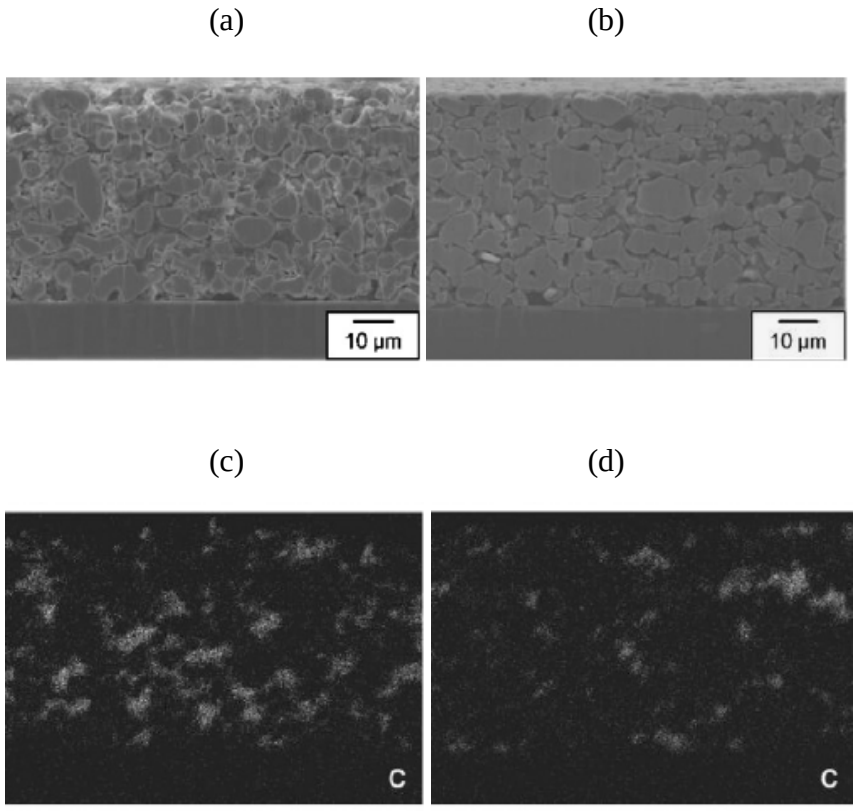

Figure 2.3. Cross-sectional SEM images of the composite electrodes: (a) from one-step process and (b) from multi-step process. (c) and (d) EDS elemental mappings of carbon [2].

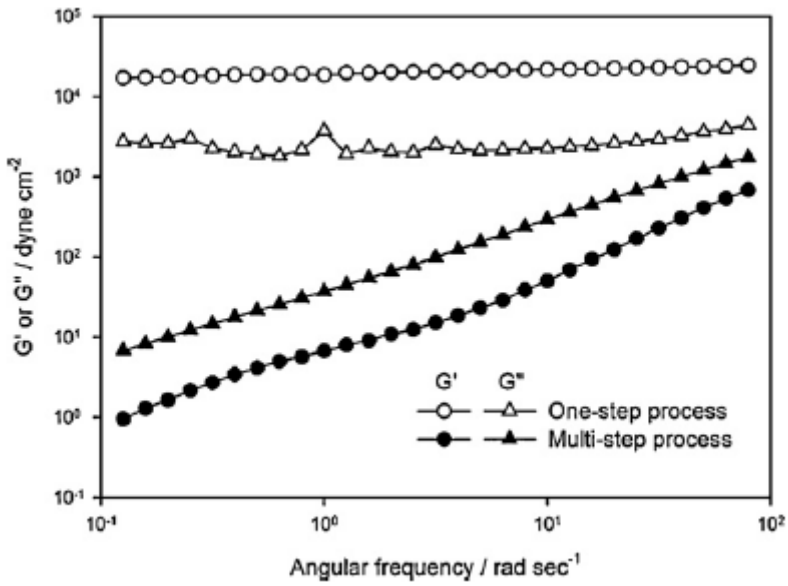

Figure 2.4. Viscoelastic modulus of the slurries prepared by two mixing processes against the angular frequency [2].

In some applications, size of large particles exceeds the upper limit of the colloidal particles because they use large particles over few micrometers. Because the gravitational force is comparable to or less than that of Brownian motions only for colloidal-sized particles, such a suspension containing large particles is not free of the gravitational effects and their behavior deviates from general colloidal theories such as DLVO theory. Preventing sedimentation can be most important factor affecting the stability of suspension in such a system.

Table 2.2. Typical composition of bimodal slurries used in industry

Application	Li-ion battery		MLCC		Conductor	
Role of particles	Main	Additive	Main	Additive	Main	Additive
Type of particles	Li(Ni,Mn,Co)O_2	Carbon black	Ni	$BaTiO_3$	Latex	ITO,
Particle size (nm)	2000~10000	20~30	300	20	300	10~20
Concentration (vol%)	20~30	0.5~2	8~15	1	2	0.05

2.3. Overview of bimodal suspensions in previous studies

Previous studies of bimodal suspension with highly size-asymmetric particles can be classified based on the relationships of surface potentials between large and small particles. The surface chemistry of nanoparticles in bimodal slurries belongs to three different categories: small particles that are attractive to each other and to large particles; repulsive to each other and to large particles; or repulsive to each other while being oppositely charged and attractive to large particles. All of the systems of bimodal suspensions can be classified within these categories. Several cases are introduced below and summarized in Table 2.3.

When repulsive small particles are added to a stable suspension of large particles, a depletion effect arises from the big size mismatch between the constituent particles, resulting in an attractive interaction between the large particles [9, 10]. Because the range of attraction is very short due to the large size asymmetry, when the volume fraction of small particles is large enough to induce strong depletion, attraction gelation or phase separation occurs [32]. For instance, this effect is known to occur when the volume fraction of small particles is more than 0.05, while the volume fraction of large particles is 0.3. If the volume fraction of large particles decreases,

more small particles are needed to induce gelation. However, for most slurries used in industry, in which only a small amount of small particles are used ($\phi_{small} < 0.03$), and as a result the concentration of small particles is far below the concentration for gelation by depletion attraction.

When the small particles are charged oppositely to large particles, electrostatic attraction arises between the large and small particles, a phenomenon that is often termed hetero-aggregation [33]. When the size ratio is small ($q = d_{small} / d_{large} < 0.07$), a very small amount of small particles leads to the formation of clusters of large particles [34], as the small particles form bridges between the large particles by forming a ring pattern on the surface of the large particles [35]. When the concentration of small particles increases, the small particles fully cover the surface of the large particles, and thus, large particles become stabilized without aggregates.

Previous studies of hetero-aggregated suspensions have focused on the kinetics or equilibrium structure. A few researchers observed changes of fluid behavior and microstructure with the addition of small particles. One of them measured the rheological properties of the suspension when the small particles induced gelation, where the size ratio was relatively large ($q = d_{small} / d_{large} \sim 0.8$) [36, 37]. In that system, the volume fraction of small

particles had to be increased up to the volume fraction of large particles to induce the gelation, and the gelation occurred over a wide concentration range. However, this result is not relevant to estimating the behavior of highly size-asymmetric particle systems.

When the small particles are electrostatically stabilized, they can stabilize the attractive micro-sized particles with very small amount [38]. This mechanism is known as nano-particle halo [39].

The systems used in the previous studies used well-stabilized nanoparticles, which are quite different from the materials used in industry. Moreover, most works on bimodal suspensions have dealt with model systems which are designed to investigate specific topics such as kinetic theory or equilibrium structure. These results are not relevant to understanding the effect of the surface chemistry of small particles on the whole fluid behavior and microstructure. Although Sun et al. [40] designed model systems to observe effects resulting from the surface chemistry of small particles, they focused on the performance of the final product, not on the fluid behavior. Therefore, in efforts to control the complex behavior of bimodal slurries, the effect of the surface chemistry of nanoparticles or the role of attractive nanoparticles has yet to be investigated systematically, considering the entire body of fluid behavior and microstructural change.

Table 2.3. Previous studies of bimodal suspension with highly size asymmetric particles

Surface of large particles	Stabilized	Not-stabilized	Stabilized
Surface of small particles	Stabilized	Stabilized	Stabilized and oppositely charged
Key phenomena	Depletion	Nanoparticle halo	Heteroaggregation
References	Biben et al. (1996) Lekkerkerker (2011)	Tohver et al. (2001)	Cerbelaud (2009)

2.4. Scaling behavior and microstructure of typical colloidal gels

When the interparticle interactions are attractive, colloidal suspensions form an elastic gel, whose modulus depends on the magnitude of attractive energy and particle volume fractions. Because elastic modulus of particulate gels is nearly independent of the frequency, a plateau modulus $G_p^{'}$ can be identified for the colloidal gels. Previous studies on the scaling behavior of colloidal gels have reported that the elastic modulus of gels follow a scaling behavior $G_p' = A\phi^{v}$ in which the power - law exponent v often has values between 3 and 5 [41-43]. A typical feature of power - law behavior is presented in Figure 2.5.

The power - law dependence is closely related to the microstructure of colloidal gels. Several models based on the fractal clusters with fractal dimension of 1.8 ~2.1 predict the power - law exponent between 3 and 5 . This result implies that the fractal-like structures which have been observed in many colloidal gels [44-46] induces the power - law behavior of elastic modulus, at least low volume fraction of particles.

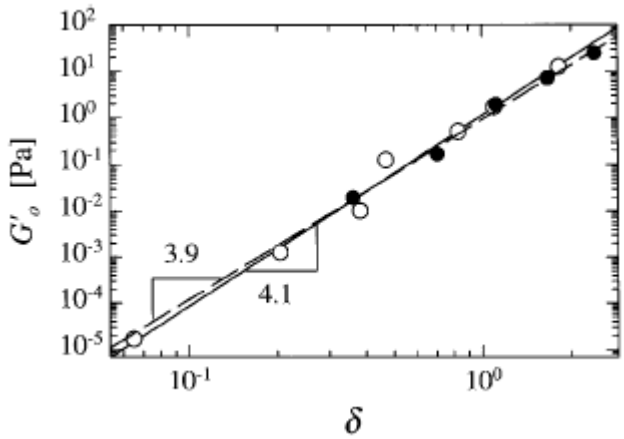

Figure 2.5. Power - law behavior of the elastic modulus as particle volume fraction ϕ (open symbols) and the magnitude of attractive energy U (solid symbols) are varied [3]. The x-axis δ is $\phi/\phi_c - 1$ for open symbols and $U/U_c - 1$ for solid symbols.

Chapter 3.

Experimental methods

3.1. Sample preparation

Raw material

Highly size asymmetric particles of charge stabilized spherical polystyrene (PS) with a diameter $d = 500\,\text{nm}$ and alumina coated silica (Ludox CL, Sigma Aldrich) with a diameter $d = 12\,\text{nm}$ were prepared. PS particles were synthesized by emulsifier-free emulsion polymerization [47].

Preparation of slurry

20 wt% of PS stock solution and 30 wt% of Ludox CL stock solution were mixed with deionized water to obtain various volume fractions. The final pH of the suspensions were adjusted using NH_4OH and HCl to 4.0 ± 0.3, 7.5 ± 0.3, and 9.0 ± 0.3. All the suspensions were mixed with a magnetic stirrer (MS-20D, Wisestir) at 100 rpm for 30 min, followed by sonication for 30 min to break large aggregates.

3.2. Measurement of suspension rheology

The rheological properties of the suspension were measured using a stress controlled type rheometer, (AR-G2, TA Instruments) at 25℃ with a cone and plate fixture. To obtain reproducible results, all measurements were performed after pre-shearing at 500 s^{-1} for 1 min and equilibration for 300 s, enough to reach a quasi-steady state, where G' remained nearly constant over time. The onset of gelation was identified by the transition from a liquid-like state with Newtonian viscosity to a solid-like state with a plateau elastic modulus [48-50].

3.3. Characterization of suspension microstructure

Microstructure was observed by cryogenic scanning electron microscopy (cryo-SEM, Tescan Mira 3 LMU FEG). The cross-section of the suspension was imaged after quenching the suspension with liquid nitrogen, sublimation at -100℃ for 30 min using the cryo-SEM sample preparation system (Quorum Technologies PP3000T), and Pt coating (10mA for 120s).

Structural analysis of the suspension at a few nanometer scale was supplemented by synchrotron small angle x-ray scattering (SAXS, Pohang Light Source Ⅱ, Korea). The incident x-ray wavelength (λ) was 0.7953 Å. For SAXS samples with thickness of 1 mm were placed in a cell with parallel mica windows.

Chapter 4.

Results and discussion

4.1. Characterization of PS/alumina coated silica suspension

4.1.1. Surface potential of PS/alumina coated silica particles at various pH

Figure 4.1.1 shows the zeta potential of the PS and the alumina-coated silica (abbreviated to Silica in the following sections) particles, which were dispersed in aqueous media of various pH. The surface potential of the PS particles was maintained to be -40 ± 10 mV at various pH, while the surface potential of the Silica particles changed with pH: +40 mV, 0 mV (IEP) and -30 mV at pH 4.0, pH 7.5 and pH 9.0, respectively. By controlling the suspension pH, only the surface of the small particles was adjusted. Therefore, the model system can describe the surface potential of small particles as oppositely charged to the large particles, negligibly charged, and highly charged at pH 4.0, pH 7.5, and pH 9.0, respectively.

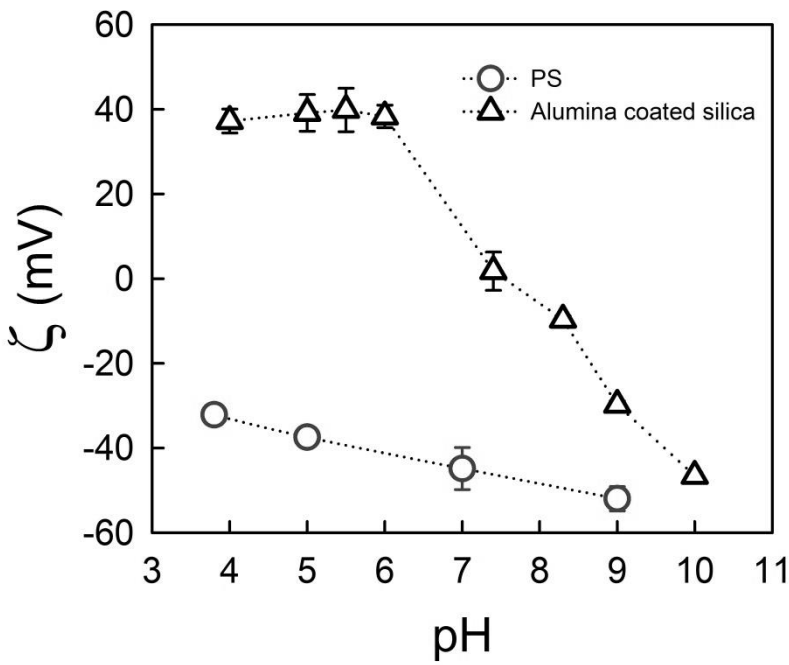

Figure 4.1.1. Zeta potentials of PS and alumina-coated silica particles as a function of pH value.

4.1.2. Stability of PS suspension

To verify the stability of the PS particles, the steady shear viscosity of PS suspensions at various volume fractions was measured and the results were plotted, in Figure 4.1.2. The colloidal suspension consisting of large particles only showed Newtonian behavior, with a constant viscosity for all different volume fractions of 2.0 vol%, 5.0 vol%, and 10.0 vol%. Because the suspensions in this study were dilute or semi-dilute, the interaction between repulsive particles did not induce any significant increase in suspension viscosity. Instead, the dependence of viscosity on particle volume fraction followed the Kreiger-Dougherty prediction for non-interacting particles [51].

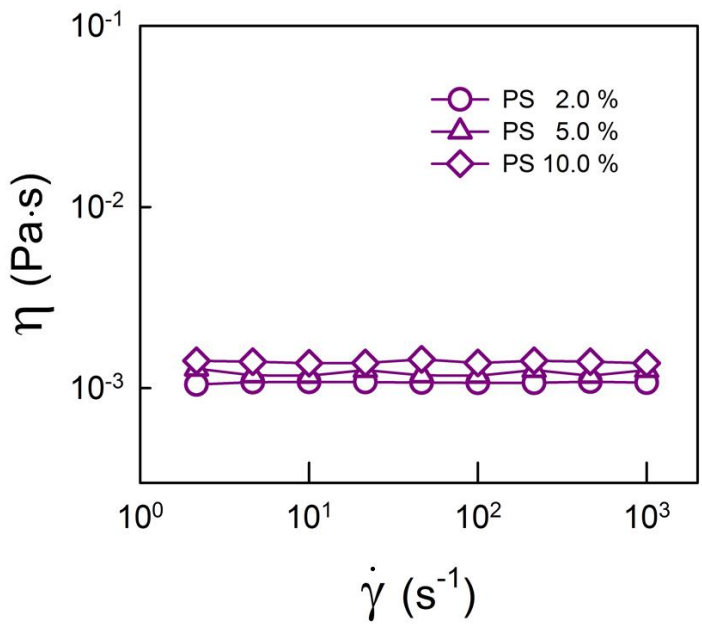

Figure 4.1.2. Steady shear viscosity as a function of shear rate for PS suspensions at various concentrations.

4.2. Effect of surface chemistry of small particles

4.2.1. Rheological behavior at various pH

To observe the change in the rheological behavior of the suspension with stabilized large particles when the various types of small particles are added, the concentration of the bimodal suspension was first fixed, corresponding to PS 5.0 vol% + Silica 0.03 vol%, and measured the steady shear viscosity of the suspensions at different pH for comparison with that of the PS 5.0 vol% suspension in Figure 4.2.1. The colloidal suspension consisting of only PS particles with 5.0 vol% showed Newtonian behavior, regardless of pH. When 0.03 vol% of Silica particles were added to the 5.0 vol% PS suspension, the rheological behavior of the bimodal suspension changed dramatically and it showed a significantly different behavior at various pH.

At pH 9.0, the suspension showed Newtonian behavior with almost the same viscosity as that of the PS suspension, which means that the addition of small particles did not affect the suspension behavior. At pH 4.0 and pH 7.5, however, the flow curves exhibited a very high viscosity at low shear and strong shear thinning.

When 1.0 vol% of small particles were added to the 5.0 vol% PS suspension, the bimodal suspensions showed Newtonian behavior with constant viscosity at both pH 4.0 and pH 9.0, while strong shear thinning was observed at pH 7.5 [Figure 4.2.1(b)]. Even at the same pH, the suspensions showed different rheological behavior with the increasing volume fraction of small particles, which indicates that both the concentration and surface chemistry of the small particles are key factors that significantly affect the rheological behavior of the bimodal suspensions.

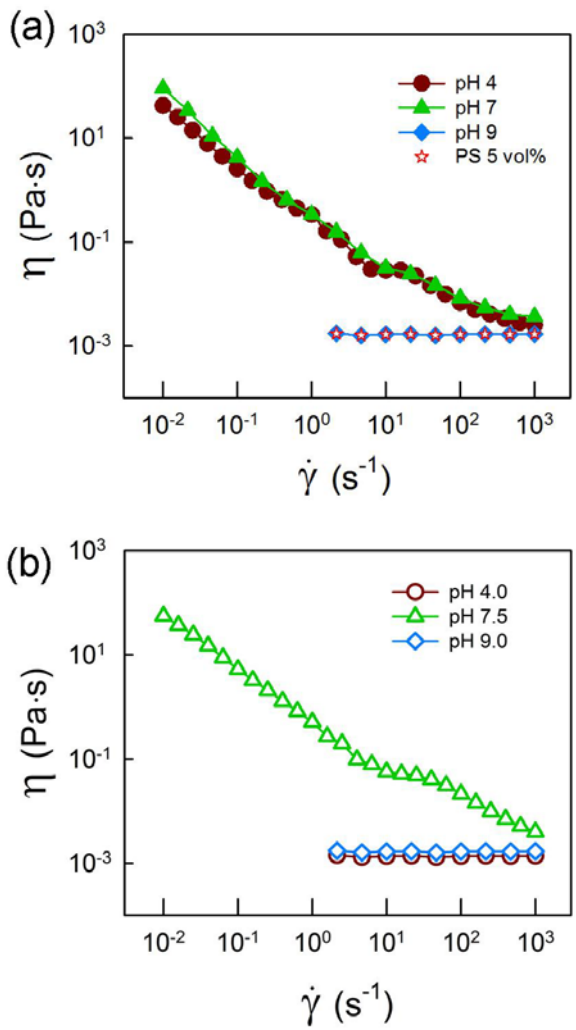

Figure 4.2.1. Effect of the surface chemistry of nanoparticles. Steady shear viscosity as a function of shear rate for (a) PS 5.0 vol% + Silica 0.03 vol% suspension, and (b) PS 5.0 vol% + Silica 1.0 vol% suspension, at various pH. Open stars represent the viscosity of the PS 5.0 vol% suspension.

Effect of adding small particles to a suspension of large particles at pH 4.0

The suspensions composed of Silica particles only show the Newtonian behavior at various concentrations when pH is 4.0, with constant viscosity of 1.31×10^{-3}, 1.60×10^{-3}, and 1.68×10^{-3} Pa.s for the suspension of 0.03 vol%, 1.0 vol%, and 3.0 vol%, respectively. When a small amount of small particles are added to the PS suspension, the flow curve changes, as in Figure 4.2.2(a). Although the suspensions composed of particles of single species show Newtonian behavior, a mixture of two types of particles show strong shear thinning behavior. This signifies that the addition of small particles induces colloidal network formation, which is verified by the frequency independent G' and G'', which is typical of a colloidal gel, as shown in Figure 4.2.2(b).

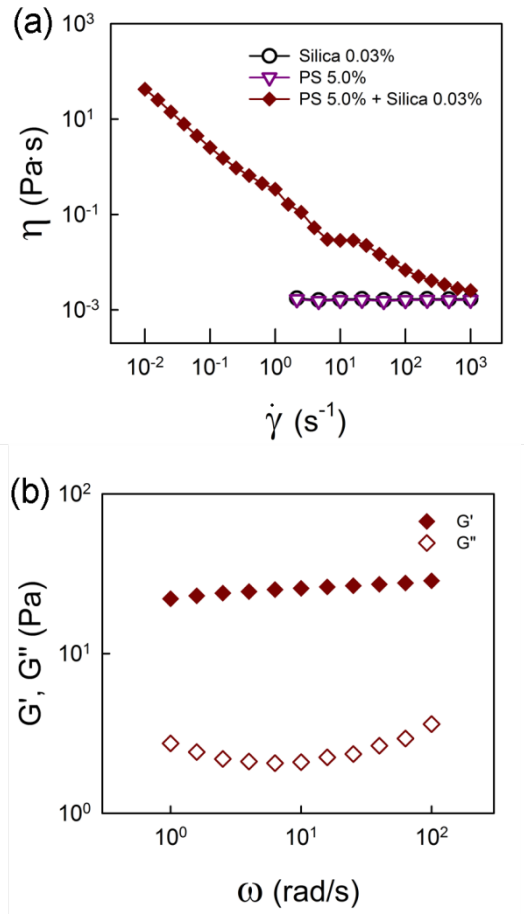

Figure 4.2.2. Effect of adding small particles (Silica) to a suspension of large particles (PS) at pH 4.0. (a) Steady shear viscosity as a function of shear rate for a suspension of 0.03 vol% Silica (open circles), 5.0 vol% PS (open triangles), and a mixture of 5.0 vol% PS and 0.03 vol% Silica (closed diamonds), (b) linear viscoelasticity as a function of frequency for a PS 5.0 vol% + Silica 0.03 vol% suspension.

Effect of adding small particles to a suspension of large particles at pH 7.5

Because small particles are mutually attractive at pH 7.5, a suspension consisting only of small particles forms a gel above the critical threshold. Silica suspensions show Newtonian behavior at a low volume fraction of particles, while they show shear thinning above 0.3 vol%, as shown in Figure 4.2.3(a). The suspensions above 0.3 vol% show gel-like behavior, with a constant G' independent of frequency as shown in Figure 4.2.3(b). From this measurement, the critical gel point of Silica particles as determined to be $\phi_c = 3 \times 10^{-3}$.

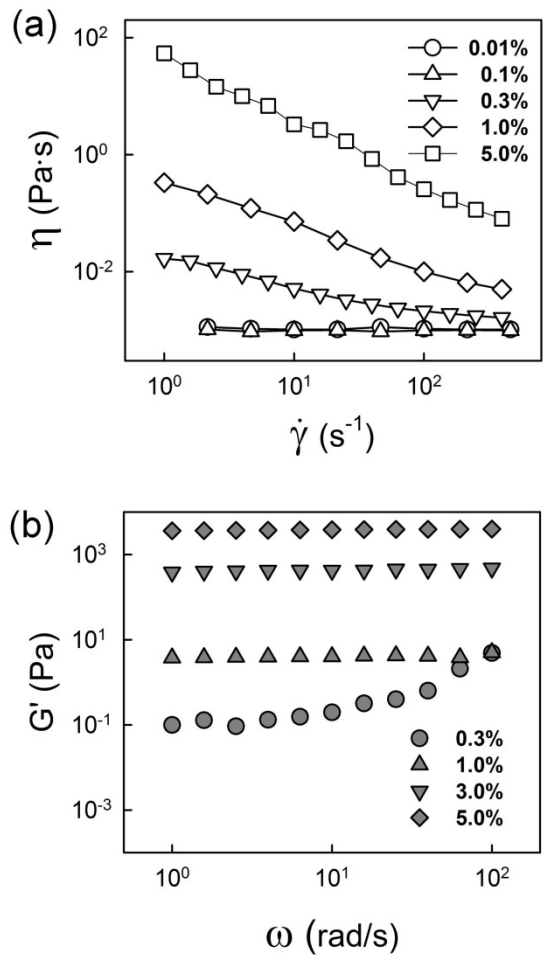

Figure 4.2.3. Rheological behavior of Silica suspension for various concentrations as indicated. (a) steady shear viscosity as a function of shear rate (b) linear viscoelasticity as a function of frequency.

When small particles are added to the suspension of large particles, the transition of the flow curve is determined by the critical gel point of small particles. When the volume fraction of small particles is lower than the critical threshold ($\phi_{small} < 3\times10^{-3}$), each suspension composed of a single species of particles shows Newtonian behavior, as in Figure 4.2.4(a). However, the mixture exhibits strong shear thinning with constant G' and G'' independent of frequency [Figure 4.2.4(b)], which means that the addition of small particles induces the formation of a network structure.

When the volume fraction of small particles is larger than the critical gel point ($\phi_{small} > 3\times10^{-3}$), the change of viscosity is not significant, as shown in Figure 4.2.4(c). However, when the large and small particles are mixed together, the G' of the mixture is much larger than that of the Silica suspension [Figure 4.2.4(d)], which signifies that large particles join the network formation together with the small particles. The increase of gel strength is not reflected on the change of viscosity because the structure breaks up during the shear flow.

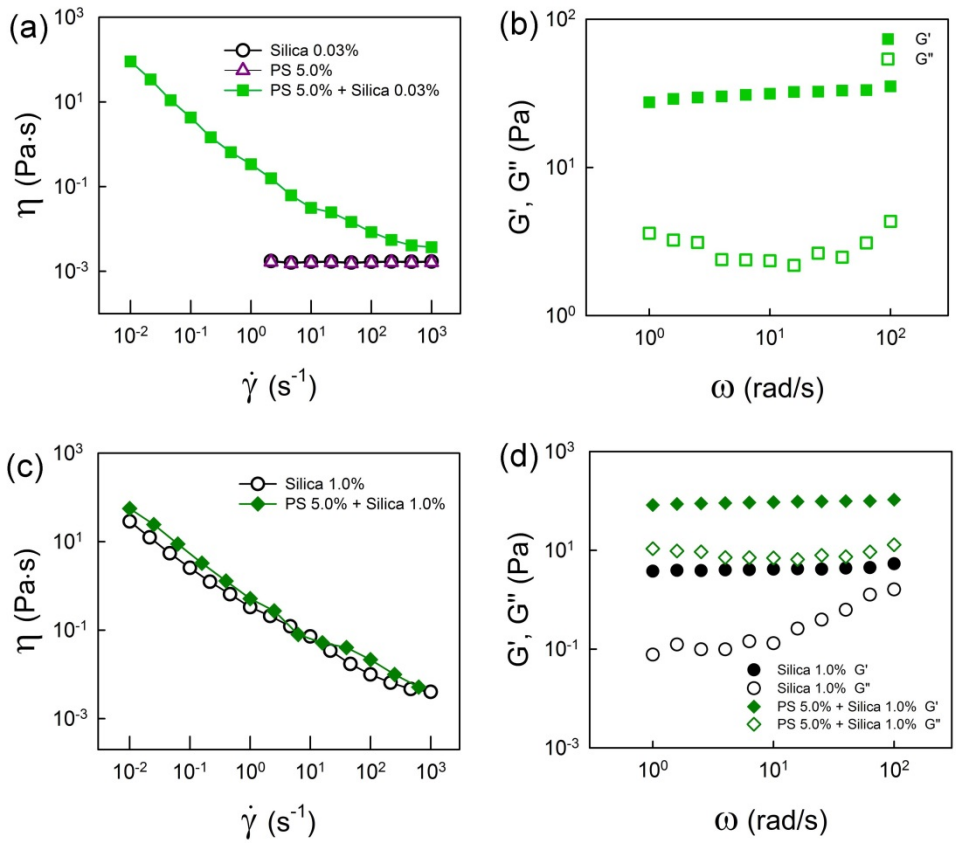

Figure 4.2.4. Effect of adding small particles (Silica) to a suspension of large particles (PS) at pH 7.5. (a) steady shear viscosity as a function of shear rate for a suspension of 0.03 vol% Silica (open circles), 5.0 vol% PS (open triangles), and a mixture of 5.0 vol% PS and 0.03 vol% Silica (closed squares), (b) linear viscoelasticity for a suspension of 5.0 vol% PS and 0.03 vol% Silica, (c) steady shear viscosity as a function of shear rate for a suspension of 1.0 vol% Silica (open circles), a mixture of 5.0 vol% PS and 1.0 vol% Silica (closed diamonds), (d) linear viscoelasticity as a function of frequency for a suspension of 1.0 vol% Silica (circles), and a mixture of 5.0 vol% PS and 1.0 vol% Silica (diamonds).

Effect of adding small particles to a suspension of large particles at pH 9.0

At pH 9.0, a suspension composed of Silica particles shows Newtonian behavior and the viscosity remains almost constant, even when the concentration of particles increases. When a small amount of small particles are added to the 5.0 vol% PS suspension, the mixture shows a Newtonian behavior with constant viscosity of 1.52×10^{-3} and 1.60×10^{-3} Pa.s for PS 5.0 vol% + Silica 0.3 vol% and PS 5.0 vol% + Silica 1.0 vol%, respectively. This indicates that the addition of small particles does not induce particle aggregation or network formation, which is in contrast to the results at pH 4.0 and pH 7.5. The Newtonian behavior with constant viscosity is maintained even though the volume fraction of added small particles increases.

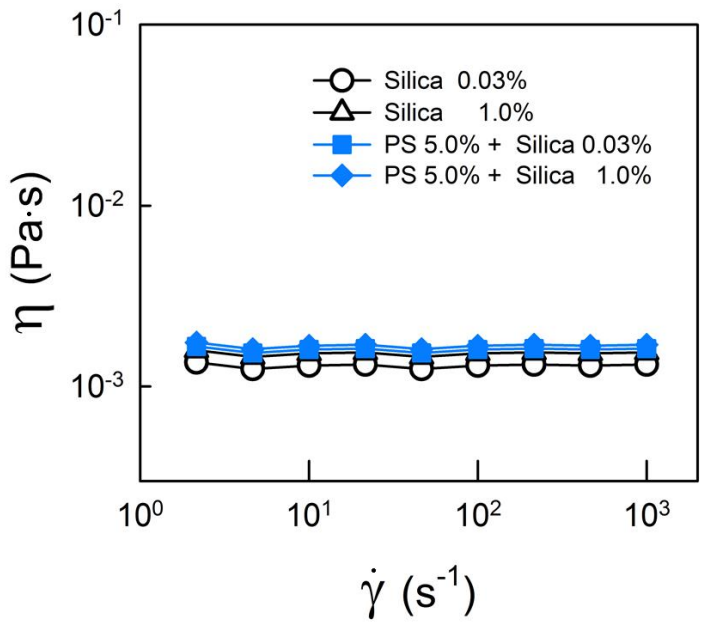

Figure 4.2.5. Effect of adding small particles (Silica) to a suspension of large particles (PS) at pH 9.0. Steady shear viscosity as a function of shear rate for a suspension of Silica suspension, PS suspension, and a mixture of PS and Silica at various concentrations.

Effect of surface chemistry on the liquid-like to solid-like transition

To understand the phase transition of bimodal suspensions, induced by the addition of nanoparticles of various surface chemistry, the fluid to gel transition was observed when the volume fraction of added small particles was increased in the range of $10^{-5} \le \phi_{small} \le 10^{-1}$ at pH 4.0, pH 7.5 and pH 9.0. A zero shear viscosity, η^* for fluid phase and the plateau elastic modulus, $G_p^{'}$ for gel phase were identified.

The phase transition, which is induced by oppositely charged nanoparticles (at pH 4.0), has two distinctive critical thresholds. As shown in Figure 4.2.6(a), a highly dispersed fluid phase is transformed into a solid network, which is followed by re-transformation to a fluid phase with an increasing volume fraction of small particles. The high size asymmetry of particle diameters results in unique phase behavior, including a narrow volume fraction range of gel phase ($10^{-4} < \phi_{small} < 10^{-3}$), while maintaining a constant modulus within each phase. The incremental increase of small particles can induce a phase transition, either a gel transition or reverse fluid transition.

The onset of gel transition which is induced by attractive nanoparticles (at pH 7.5) is also observed in Figure 4.2.6(b). A highly dispersed fluid phase is transformed into a solid network above the critical threshold ($\phi_{small} > 10^{-4}$). After the gel transition, the plateau modulus G'_p increases as the volume fraction of small particles increases. This is distinctive from the critical onset of gelation of typical colloidal gels, where the viscosity diverges and the elastic modulus increases exponentially in the vicinity of a critical gel point [52-55].

When the repulsive small particles are added, the suspension shows Newtonian behavior over the whole range of small particle volume fractions [Figure 4.2.6(c)], which means that the gel transition does not occur and the suspension remains in a fluid state over the wide range of small particle volume fractions covered in this study. The viscosity is nearly unchanged at small volume fractions.

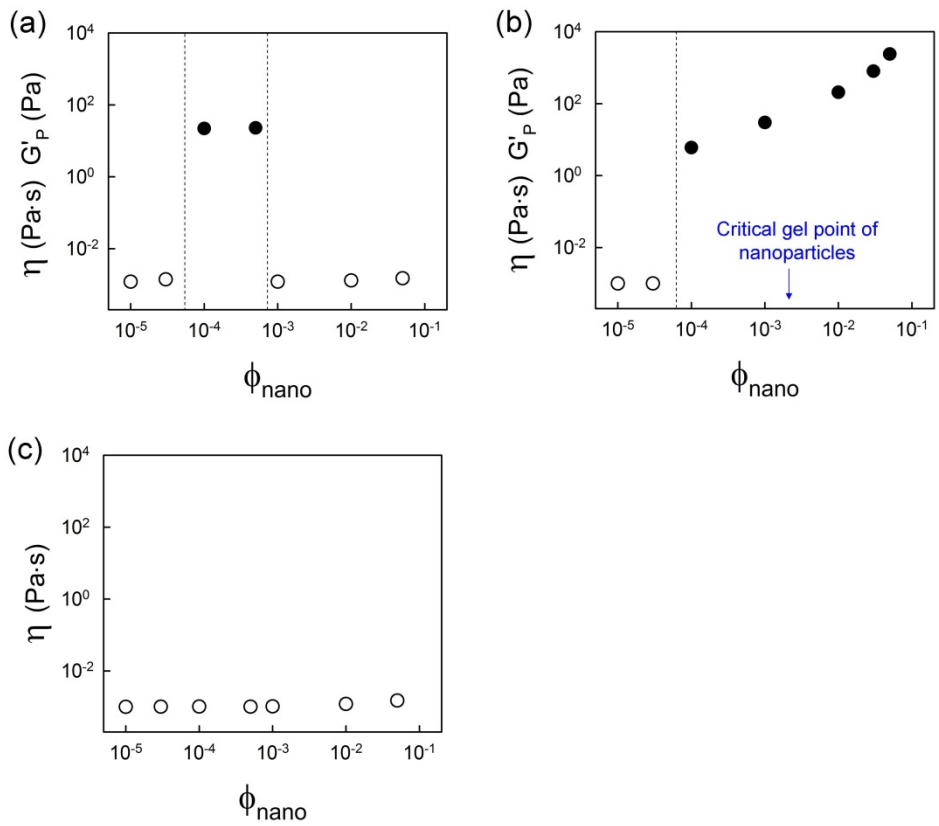

Figure 4.2.6. Effect of nanoparticle concentration on the fluid to gel transition of bimodal suspensions ($\phi_{large} = 0.05$ fixed) at (a) pH 4.0 (b) pH 7.5 (c) pH 9.0. Fluid phase exhibits zero shear viscosity (open circles) and gel phase exhibits plateau elastic modulus (closed circles).

4.2.2. Microstructural analysis

The microstructure of the PS 5.0 vol% + Silica 0.03 vol% suspension at pH 4.0, which is in a gel phase, is shown in Figure 4.2.7(a). The small particles are adsorbed onto the surface of large particles. Because the large particles are strongly repulsive to each other, they do not form a network structure directly, but are bridged by the small particles [Figure 4.2.7(b)]. This bridging allows the repulsive large particles to form a spanning network and to show gel behavior.

At pH 7.5, the features of the microstructure were distinctive for each volume fraction of small particles. When the volume fraction of small particles was below the critical gel point of small particles, as represented by the PS 5.0 vol% + Silica 0.03 vol% suspension, the large particles were bridged by the small particles which led to the formation of gels, as shown in Figure 4.2.7(c). The gel structure looks similar between pH 4.0 and pH 7.5 in that the bridging by small particles is a key mechanism which induces the formation of particle networks. However, at pH 7.5 the large particles are bridged by clusters of small particles, not by individual small particles as with pH 4.0. This causes the distance between large particles at pH 7.5 to be larger than the distance at pH 4.0.

When the volume fraction of small particles was higher than the gel point of small particles, represented by the PS 5.0vol % + Silica 1.0% suspension, the clusters of small particles fully covered the surface of the large particles, which implies that the large particles were a part of the spanning networks formed by the small particles, as shown in Figure 7(d). Because the large particles are the part of the spanning networks, the bimodal suspension shows higher elastic modulus than the Silica suspension, as shown in Figure 4.2.7(d).

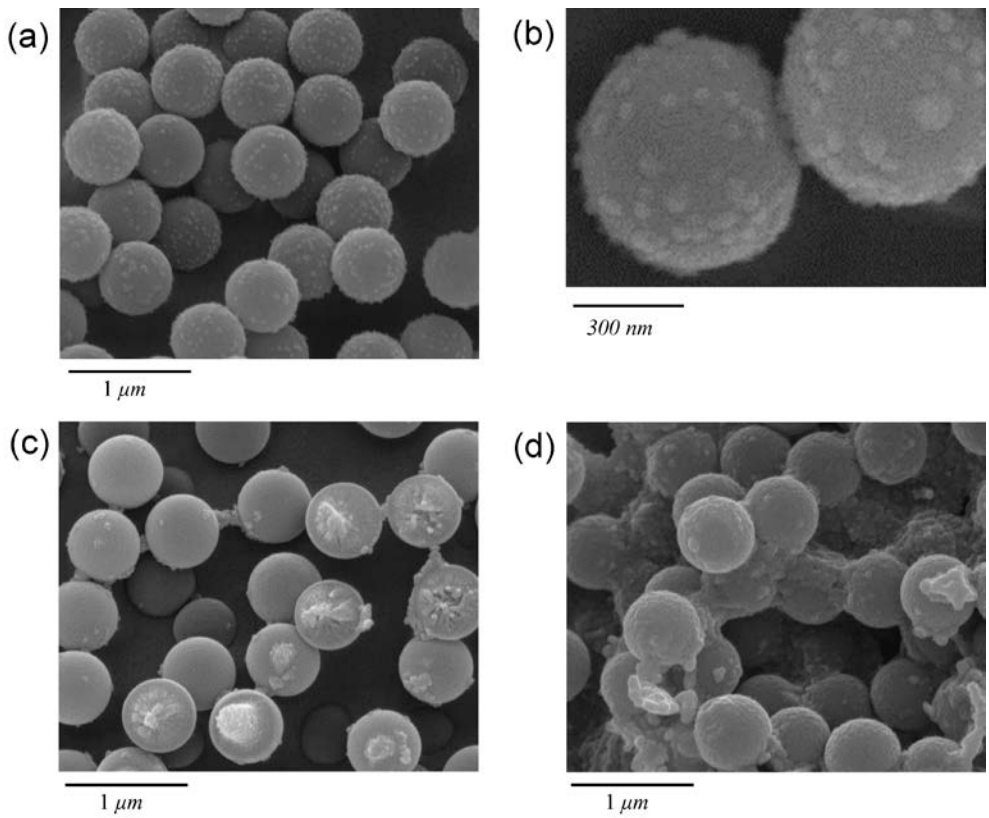

Figure 4.2.7. Microstructure of bimodal gels. (a) and (b) PS 5.0 vol% + Silica 0.03 vol% suspension at pH 4.0, (c) PS 5.0 vol% + Silica 0.03 vol% suspension at pH 7.5, (d) PS 5.0 vol% + Silica 1.0 vol% suspension at pH 7.5.

4.2.3. Origin of nanoparticle induced gelation

The origin of particle networks and phase behaviors can be understood by considering the surface potentials between constituent particles. Because the particles are dispersed in an aqueous medium, the balance between the van der Waals attraction and electrical double layer interaction determines the interaction between the particles. In the Derjaguin, Landau, Verwey and Overbeek (DLVO) theory, the potential energy of the van der Waals attraction and electrical double layer interaction are summed to obtain the total interaction potential energy between constituent particles.

$$U_{total} = U_{vdW} + U_{el} \qquad (1)$$

To describe the particle interactions in bimodal suspensions, the total interaction energy for large - large, small - small, and small - large particles has to be calculated. For two different sizes of spherical particles, the potential energy of van der Waals attraction is given by [56]

$$U_{vdW} = -\frac{A}{6}\left(\frac{2R_1R_2}{f_1} + \frac{2R_1R_2}{f_2} + \ln\left(\frac{f_1}{f_2} \right) \right),$$

$$f_1 = h^2 + 2R_1h + 2R_2h,$$

$$f_2 = h^2 + 2R_1h + 2R_2h + 4R_1R_2 \qquad (2)$$

where R_1 and R_2 are the radii of the two particles, h is the particle surface separation, and A is the Hamaker constant which depends on the polarizability of the particles and the solvent. This equation holds for all sets of interactions (large - large, small - small, small - large). The Hamaker constants chosen for PS - PS, Silica - Silica, PS - Silica interactions in water were $A_{11} = 1.37 \times 10^{-20} J$, $A_{22} = 2.75 \times 10^{-20} J$, and $A_{12} = \sqrt{A_{11}A_{22}} = 1.94 \times 10^{-20} J$, respectively [56].

The potential energy of the electrical double layer interaction for unlike particles is given by [57]

$$U_{el} = \pi\varepsilon_r\varepsilon_0\left(\frac{kT}{e}\right)^2 \frac{R_1R_2}{R_1+R_2+h}\left[\left(y_1+y_2\right)^2 \ln\left(1+e^{-\kappa h}\right)+\left(y_1-y_2\right)^2 \ln\left(1-e^{-\kappa h}\right)\right],$$

$$y_1 = \frac{e\psi_1}{kT}, \quad y_2 = \frac{e\psi_2}{kT}. \qquad (3)$$

where ψ is the surface potential of each particle, as approximated by the measured zeta potential, ε_r is the relative permittivity of the intervening

medium, ε_0 is the permittivity of free space, κ is the inverse Debye screening length, which is given by ,

$$\kappa = \left(\frac{\sum_j \left(z_j e \right)^2 n_j}{\varepsilon_r \varepsilon_0} \right)^{1/2}, \qquad (4)$$

where n_j is the concentration in number per unit volume of j-th type of ion, and e is the elementary charge.

The Debye screening length is calculated by the ion concentration (the electrolyte is assumed to be symmetrical with single valence), which is estimated by measuring the dispersion conductivity [40]. The dispersion conductivities, estimated electrolyte concentrations, and the corresponding electrical double layer thickness calculated by Eq. (4) are given in Table. 4.1.

Although Eq. (3) is valid only for small κh and $\psi < 25mV$, many previous studies have verified that it gives a reasonable approximation even for a higher surface potential, 30~40mV, to qualitatively describe the particle interaction [35, 40]. Also, because the formula for high κh shows negligible difference with Eq. (3), at least for this system parameters, Eq. (3) was used to calculate the interaction of large-large and small-large particles.

The total DLVO interaction potential energies for PS - PS, PS - Silica, and Silica - Silica in aqueous media at pH 4.0, pH 7.5, and pH 9.0 are presented in Figure 4.2.8. At pH 4.0, as shown in Figure 4.2.8(a), the energy barriers for PS - PS and Silica - Silica are high due to the electrostatic repulsion, while that of PS - Silica is attractive, because the surface of the Silica particles is oppositely charged on the surface of the large particles. This result indicates that particle aggregation occurs only between large and small particles at pH 4.0. At pH 7.5, the PS - PS interaction is unchanged from the previous calculation, but the interactions for PS - Silica and Silica - Silica are dominated by the van der Waals attraction [Figure 4.2.8(b)]. At pH 9.0, the electrostatic repulsion dominates for all three types of interactions. These results verify that the interactions between large particles do not change with pH, but the interactions involved with small particles are significantly different.

Table 4.1. The dispersion conductivity, estimated electrolyte concentration (assumed to be symmetrical single valance type), and corresponding electrical double layer thickness

Dispersion	Conductivity (mS)	Ion concentration (M)	Electrical double layer thickness (nm)
Silica/PS, pH 4.0	0.23	0.0023	6.4
Silica/PS, pH 7.5	0.32	0.0032	5.4
Silica/PS, pH 9.0	0.33	0.0032	5.3

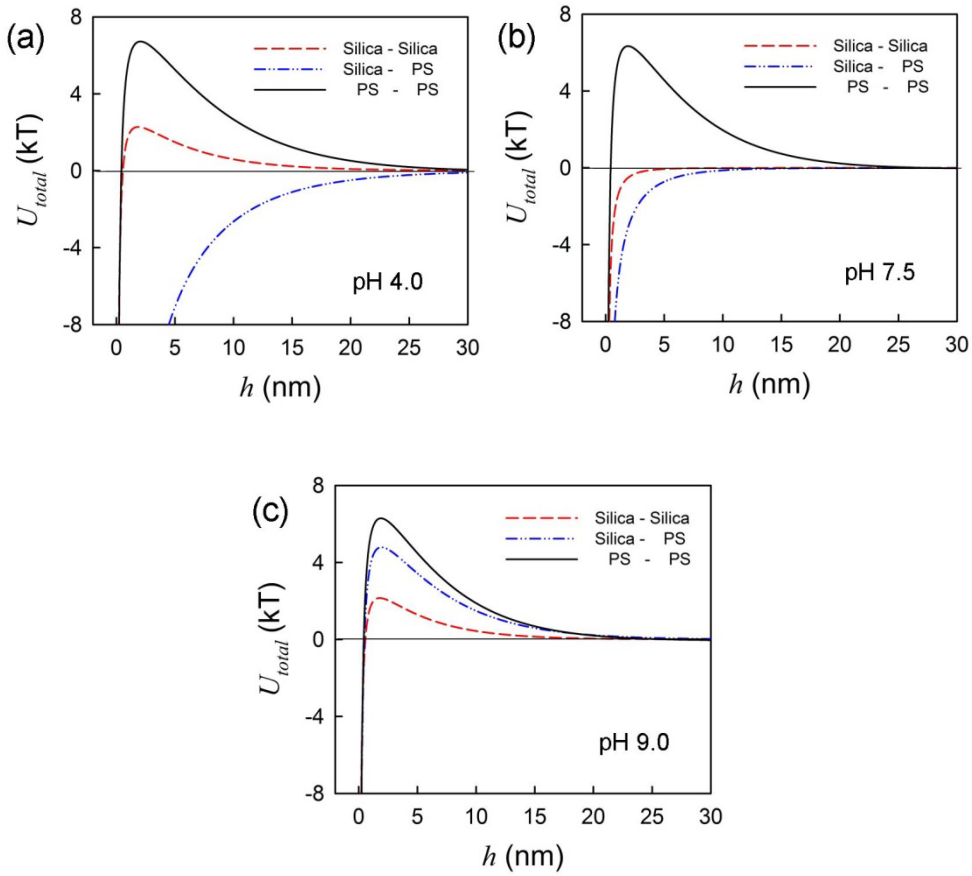

Figure 4.2.8. DLVO interaction potentials as a function of the center to center separation distance between the particles at (a) pH 4.0, (b) pH 7.5, and (c) pH 9.0. The data for PS - PS in relation to the actual values are reduced by 15 times, for comparison.

4.2.4. Phase diagram

From the potential energy evaluation and experimental observations, the phase and microstructure changes in the suspension of highly size asymmetric particles can be explained as follows. When the small particles have the opposite charge of the large particles (at pH 4.0), the following phase transitions occur: from the fluid to the bridging gel (short), and to fluid again with an increase in the volume fraction of the small particles. Below a lower critical concentration, $\phi_{small} < 10^{-4}$, the amount of small particles is too low to connect the large particles to form a gel. At intermediate particle volume fractions, $10^{-4} < \phi_{small} < 10^{-3}$, the large particles are bridged by the adsorbed small particles and form gels. Because the small particles are repulsive to each other, as in Figure 4.2.8 (a), the individual small particles are adsorbed onto the surfaces of the large particles, which results in short range bridging. Above the upper critical concentration of small particles, $\phi_{small} > 10^{-3}$, the small particles fully cover the surfaces of the large particles and the large particles are stabilized by the electrostatic repulsion of the adsorbed Silica particles.

When the small particles are not stabilized (at pH 7.5), the following phase transitions occur: the fluid transitions to a bridging gel (long), and to a dense gel as the volume fraction of small particles increases. Below a lower critical concentration, $\phi_{small} < 10^{-4}$, the amount of small particles is too low to connect the large particles to form a gel. At an intermediate particle volume fraction, $10^{-4} < \phi_{small} < 3 \times 10^{-3}$, large particles form gels which are bridged by the clusters of small particles. Because the small particles are attractive to each other due to the van der Waals force, as shown in Figure 4.2.8 (b), the clusters of small particles are adsorbed onto the surfaces of the large particles, which results in long range bridging. Above an upper critical concentration of small particles, $\phi_{small} > 3 \times 10^{-3}$, the clusters of small particles connect the large particles by fully covering the surfaces of the large particles, and this phase is termed a dense gel.

When the small particles are stabilized (at pH 9.0), the phase remains in the fluid state for the entire volume fraction range of small particles, $10^{-5} < \phi_{small} < 10^{-1}$. As in Figure 4.2.8 (c), the repulsive force dominates the interaction between the particles, which results in good dispersion. Because the size ratio is very small, depletion can be induced if the volume fraction of small and large particles increases much more. However, the range of

concentration covered in this study is comparable to those of slurries used in practice, and is much lower than the range where depletion takes place.

Several types of gel phases in the bimodal suspensions were distinguished and plotted in a phase diagram, presented in Figure 4.2.9, in which the fluid to gel transition was determined by the rheological method and the gel phase was evidenced by the microstructure. The x-axis represents the surface chemistry of the small particles, which are classified as oppositely charged, not stabilized; and stabilized nanoparticles, corresponding to pH 4.0, pH 7.5, and pH 9.0, respectively. The y-axis represents the volume fraction of added small particles. Although this phase diagram is limited to a fixed concentration (5.0 vol%) of large particles, it is expected that it exhibits representative phase behaviors which can be observed in the suspensions of highly size-asymmetric particles.

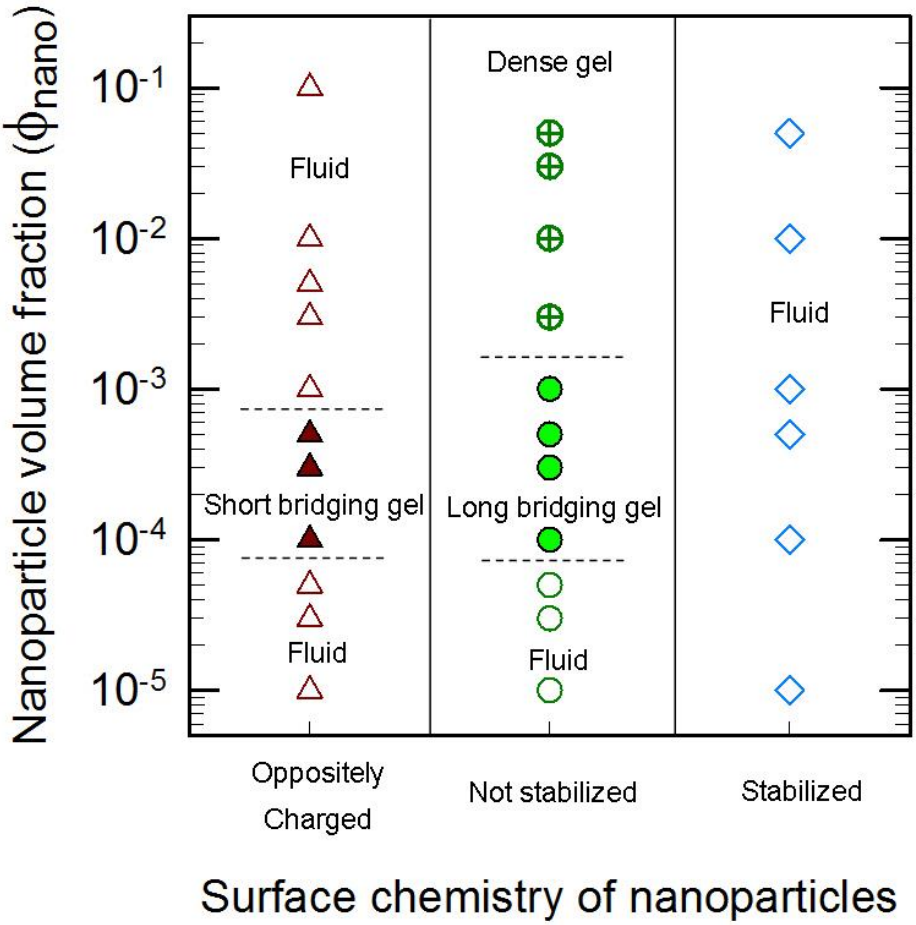

Figure 4.2.9. Phase diagram of bimodal suspensions with high size ratio of particles ($q = d_{small} / d_{large} = 0.02$). The concentration and surface potential of the large particles were fixed at 5.0 vol% and electrostatically stabilized, respectively. Open symbols (triangles, circles, and diamonds) represent a fluid phase, closed triangles represent a short bridging gel, closed circles represent a long bridging gel, and crossed open circles represent a dense gel.

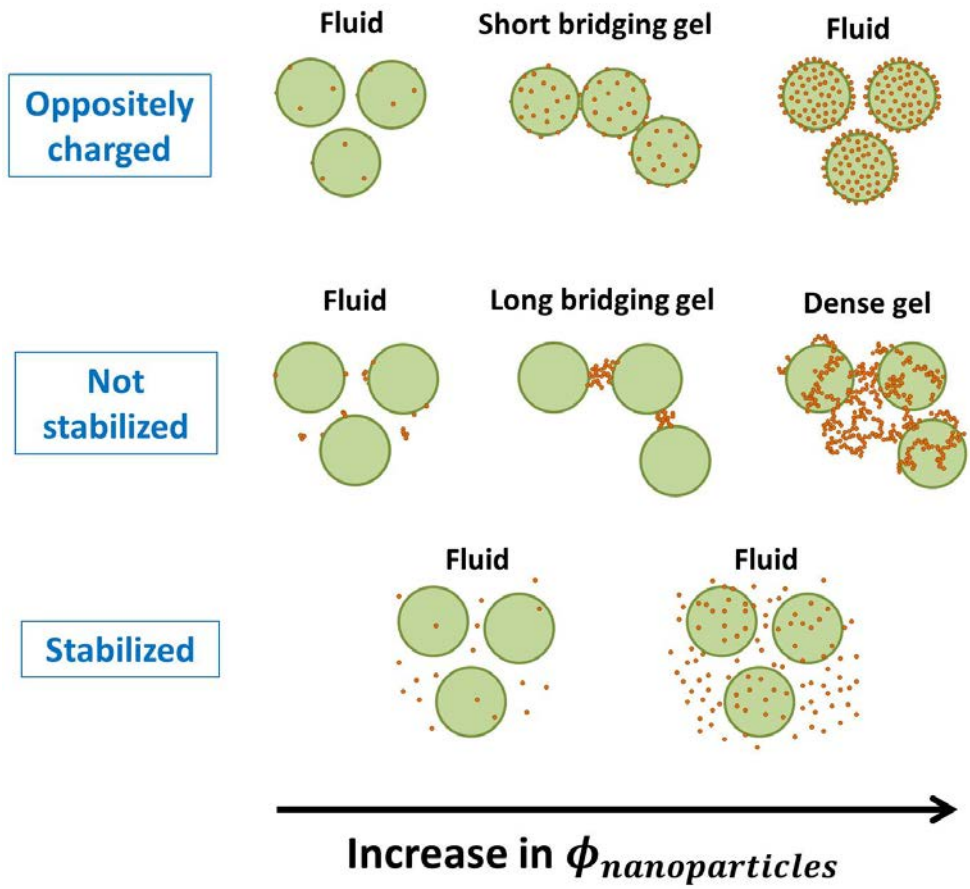

Figure 4.2.10. Schematic diagram of microstructural changes in bimodal suspensions with small size ratio of particles.

4.3. Attractive nanoparticle induced gelation

4.3.1. The onset of gelation

The onset of bimodal gelation was determined from the rheological behavior of the suspension. As shown in the left plot of Figure 4.3.1, when the volume fraction of added small particles was too low ($\phi_{small} < 10^{-4}$) , the bimodal suspension exhibits a Newtonian behavior, indicating no spanning network is being formed. After the amount of added small particles exceeds a critical threshold $\phi_{small} > 10^{-4}$, the bimodal suspension shows gel-like behavior, showing a constant G' independent of frequency, as in the right of Figure 4.3.1. The amount of small particles required for the onset of gelation is much lower than the critical gel point of small particles ($\phi = 3 \times 10^{-3}$).

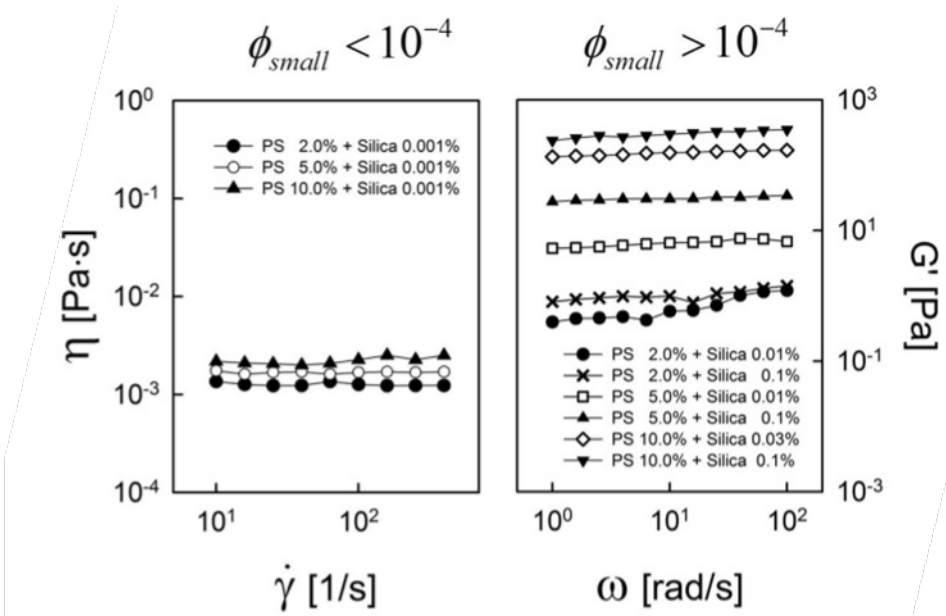

Figure 4.3.1. Rheological properties for the bimodal suspensions (PS+Silica) at variouse concentrations.

4.3.2. Scaling behavior

To compare the mechanical properties between bimodal gels formed by the addition of small particles and colloidal gels consisting only of small particles, the scaling behavior of elastic modulus G' on total volume fraction of the particles was explored. Because G' is nearly independent of the frequency, a plateau modulus $G_p^{'}$ could be identified for the colloidal gels. The elastic modulus of gels of monodisperse small particles followed a scaling behavior $G_p' = A\phi^v$ with an exponent of 4.6 ± 0.1, in good agreement with the scaling observed for a variety of previously reported colloidal gels, in which the power law exponent v often has values between 3 and 5 [58].

In contrast, the bimodal gels that resulted from the addition of small particles were not described by a single power law relationship, but rather had two regions of vastly different exponents. This is clearly observed in Figure 4.3.2 where small particles were added to fixed concentration PS suspensions of 2.0 vol%, 5.0 vol%, and 10.0 vol%, respectively. At high concentration of small particles, the exponents of the bimodal gels are the same as those of monodisperse colloidal gels, 4.6 ± 0.1. Each data set of bimodal gels with PS loading of 2.0 vol%, 5.0 vol%, and 10.0 vol% has the

same exponent in this region. On the other hand, at low concentration of small particles, the bimodal gel shows a significant difference from the typical colloidal gels, with a power - law exponent much larger than 3 - 5. Because various models based on fractal aggregates predict exponents between 3 and 5, the results of this study suggest that the microstructure of the bimodal gels at low concentration of small particles is significantly different from a fractal structure. Such a distinct exponent demonstrates that the elastic moduli of bimodal gels cannot be scaled onto a single master curve. This conclusion deviates from previous reports on colloidal gels whose elastic moduli scale onto a single curve with respect to the volume fraction of the particles [59].

Interestingly, for all the sets of bimodal gels, the volume fraction of small particles was the same, $\phi_{small} = 3 \times 10^{-3}$ at the transition point of the two distinct curves, and that volume fraction is identical to the gel point of monodisperse small particle suspensions. This result presents a different point of view than previous research on binary colloids, in which the relative contents of two different particles have been considered to be the main parameter that determines mechanical behavior [13]. In this system, the transition of mechanical behavior is determined solely by the small particles' ability to form gels.

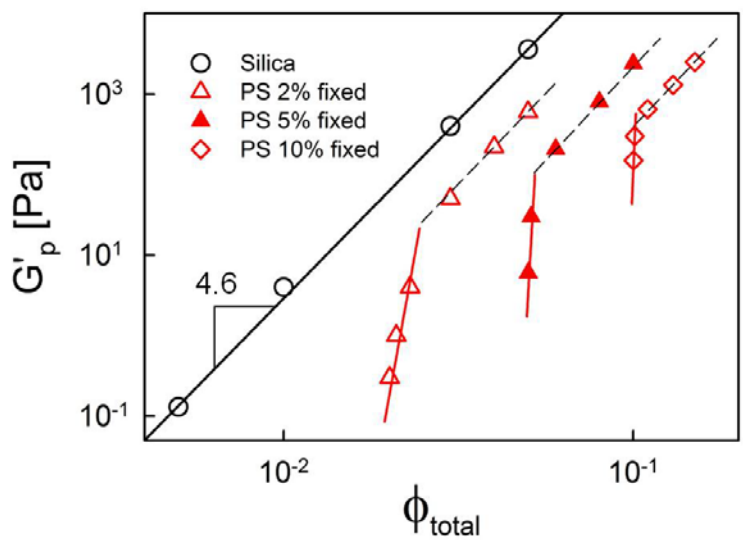

Figure 4.3.2. Power - law scaling of plateau modulus with volume fraction of total particles for the Silica suspension (open circles) and the bimodal suspensions of fixed PS concentration at 2.0 vol% (open triangles), 5.0 vol% (closed triangles), and 10.0 vol% (open diamonds). Solid lines and dashed lines are the results of fits to power - law equations, $G'_p = A\phi^v$. For bimodal suspensions, fitting was performed separately for the data in the high and low exponent regions.

4.3.3. Microstructural analysis

Using Cryo-SEM and SAXS, the structure of the bimodal gels and the origin of their rheological behavior were explored. Two representative samples were chosen, one each from the high exponent region (low small particle loading) and low exponent region (high small particle loading), corresponding to PS 5.0 vol% + Silica 0.1 vol% and PS 5.0 vol% + Silica 1.0 vol% samples.

First, the microstructures of the small particles were analyzed by SAXS to understand their morphology at a few nanometers scale. In the SAXS experiments, although both large and small particles exist in the fluid only the structure formed by the small particles was observed, as the operating q-range is $q < 0.06$ nm^{-1}. As shown in Figure 4.3.3, they exhibit a power - law behavior whose exponent gives an estimate of the fractal dimension, with values of 2.1 and 1.8 for PS 5.0 vol% + Silica 0.1 vol% and PS 5.0 vol% + Silica 1.0 vol% samples, respectively. A similar decrease of fractal exponent in a scattering experiment was observed with increasing particle concentration in a previous study [60]. Therefore, from the microstructure of the two representative samples at high and low exponent regions, it is confirmed that the small particles form aggregates with a fractal structure

regardless of their concentrations.

Although the small particles in the two samples had similar fractal clusters, distinctly different morphology was found between the two samples at micrometer scale in cryo-SEM images. At high small particle loading ($\phi_{small} > \phi_{small,gel}$), the large particles formed a network structure, as in Figure 4.3.4 (a). This resembles the fractal structure of typical colloidal gels which have been reported previously [61, 62]. At low small particle loading ($\phi_{small} < \phi_{small,gel}$), on the other hand, the large particles did not form a fractal-like structure and were just interspersed throughout the fluid [Figure 4.3.4 (b)].

The inset image of Figure 4.3.4 (a) shows that the clusters of small particles fully cover the surfaces of the large particles, which implies that the large particles are a part of the space-filling network formed by small particles. Therefore, the microstructure of high small particle loading exhibits fractal networks composed of both small and large particles, leading to the power - law exponent between 3 - 5.

At low small particle loading, although the large particles seem to be well-dispersed, a closer examination, as shown in the inset of Figure 4.3.4 (b), reveals that the small particles are bridging these large particles in the medium. This bridging allows the interspersed large particles to form a

spanning network and exhibit gel behavior. The small particles form fractal clusters as seen in Figure 4.3.3, and the discrete fractal clusters of small particles simply bridge the large particles: the large particles do not form a fractal structure, which explains why the rheological behavior of the samples with low small particle loading does not follow the typical power law behavior of previously reported colloidal gels.

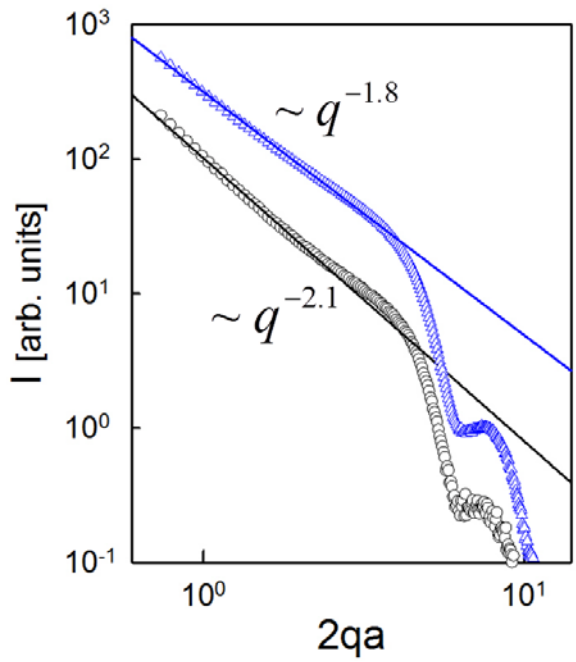

Figure 4.3.3. Microstructure of two representative samples, one each from a high exponent region (low small particle loading) and a low exponent region (high small particle loading). SAXS data of PS 5.0 vol% + Silica 1.0 vol% (open circles) and PS 5.0 vol% + Silica 0.1 vol% (open triangles) in which solid lines are fitted to the equation $I \sim q^{-D_f}$.

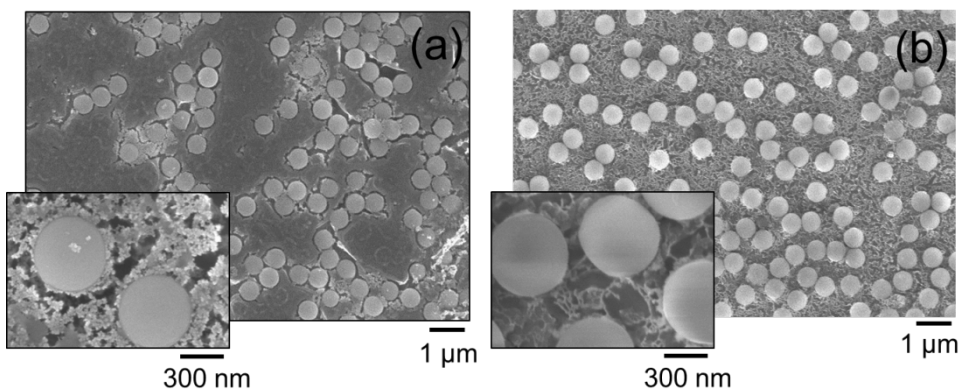

Figure 4.3.4. Microstructure of two representative samples, one each from a high exponent region (low small particle loading) and a low exponent region (high small particle loading). (a) Cryo-SEM image of PS 5.0 vol% + Silica 1.0 vol%, (b) cryo-SEM image of PS 5.0 vol% + Silica 0.1 vol%.

Additionally, the SEM images of identical samples after drying provide us with another evidence that supports the explanation of the different microstructures of the two samples. At high small particle loading, large particles form a fractal-like structure, surrounded by space-filling clusters by small particles [Figure 4.3.5 (a)]. In contrast, large particles just connected by clusters of small particles and are arranged relatively in order Figure 4.3.5 (b) for sample with the high small particle loading.

Interestingly, this morphology is reminiscent of ternary fluid-fluid-solid systems, in which addition of interfacially active particles onto blends of immiscible polymers with droplet/matrix morphology have distinct microstructural effect with amount of particle loading [63]. Active particles bridge the droplets at low particle loading, while active particles form a connected network while covering the droplet thoroughly at high particle loading. The authors suggested that both clusters could form a spanning network, leading to a transition from fluid to gel in rheological behavior. Although the ternary system used for their study is different from our fluid-solid-solid ternary system, such similarity in the observed mechanism of the microstructural behavior provides another evidence that supports this explanation of the structural and mechanical properties.

The microstructure of high small particle loading sample exhibits fractal

network of the small particle that incorporates the large particles, in accordance with its power - law behavior with exponent between 3~5. However, in the low small particle loading sample, the large particles formed an interspersed state with the small particles bridging these particles. Such microstructure, which is vastly different from the fractal aggregates, explains why the rheological behavior of the samples in low small particle concentration region does not follow the typical power law behavior of previously reported colloidal gels. Because the composition of many industrial slurries are in the range of high exponent region, this study demonstrates that understanding of such non-fractal gelation and development of new method to predict its mechanical behavior is crucial to solving many of the issues in the industrial application of colloids.

(a)

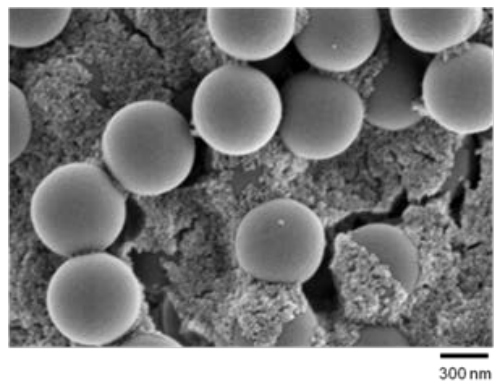

(b)

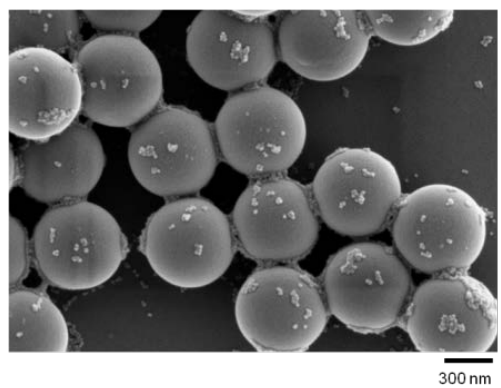

Figure 4.3.5. FE-SEM image of drying film for a suspension of (a) PS 5.0 vol% + Silica 1.0 vol%, (b) PS 5.0 vol% + Silica 0.1 vol%.

As the particles are dispersed in aqueous medium, the balance between the electrical double layer force and the van der Waals force determines the particle interaction. The interaction between the same species of particles is clear - the electrical double layer repulsion dominates between highly charged large particles and the van der Waals attraction dominates between neutral small particles. As in Figure 4.3.4, the attractive interaction plays a dominant role between large and small particles. According to a model that calculates the electrical double layer repulsion between dissimilar particles [57], the electrostatic repulsion does not arise between large and small particles, even though the Debye length of large particles changes. In addition, the behavior of bimodal gels in this study is observed at very low volume fraction of small particles, thus it is distinguishable to depletion gels which is observed at higher volume fraction in the region of $\phi_{small} \geq 0.07$ for $\phi_{large} = 0.2$ at various size ratios [32]**.** Thus the van der Waals attraction is the dominant force that drive the gel formation.

4.3.4. Phase diagram

Two types of bimodal gels were distinguished and plotted in the phase diagram in Figure 4.3.7, which is divided into three regions: (a) a fluid consisting of discrete clusters of small and large particles below the critical value of small particle volume fraction, $\phi < \phi_{L,C}$, (b) a bimodal gel, in which small particle clusters bridge large particles at intermediate small particle volume fraction, $\phi_{L,C} < \phi < \phi_{U,C}$, (c) a bimodal gel above the upper critical value of small particle volume fraction, $\phi > \phi_{U,C}$, in which both small and large particles form fractal structures. Below a lower critical concentration of small particles, $\phi_{L,C}$, the amount of small particles is too low to connect the large particles to form a spanning network. Each remain in the fluid state, with discrete clusters of large and small particles. When the fraction of small particles becomes greater than the lower critical value of small particle volume fraction, $\phi > \phi_{L,C}$, the large particles form a non-fractal network with the small particles, altering the rheological behavior from liquid-like to gel-like. The bimodal gels formed in this region have much larger power - law exponent than the 3 - 5 which is typical for fractal gels. The lower critical concentration is the minimum volume fraction of

small particles required to connect the large particles to form a gel, and it increases with the volume fraction of large particles.

Above the upper critical concentration of small particles, $\phi > \phi_{U,C}$, the transition to bimodal gel structure occurs, where the power - law exponent is reduced to a value between 3 and 5. While the $\phi_{L,C}$ increases with the volume fraction of large particles, the $\phi_{U,C}$ is independent of the fraction and remains equal to the gel point of small particles. Therefore, the region of high exponent bimodal gels in the phase diagram decreases with the increase in the volume fraction of large particles. It is expected that it would be difficult to form high exponent bimodal gels at high concentration of large particles.

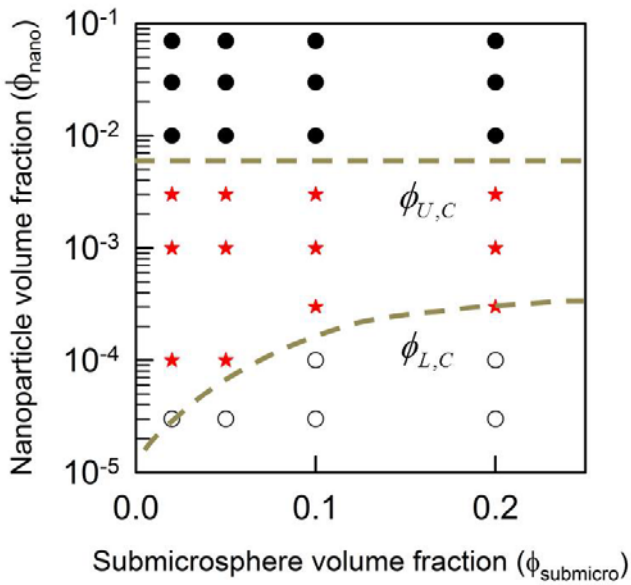

Figure 4.3.6. Phase diagram of bimodal suspensions of repulsive large particles and attractive small particles ($d_{large} = 500$ nm and $d_{small} = 12$ nm). Open circles represent a fluid consisting of discrete clusters of large and small particles, closed stars represent a bimodal gel in which small particle clusters bridge large particles, and closed circles represent a bimodal gel in which both small and large particles form fractal structures. The lower and upper dashed lines illustrate the experimentally observed critical boundary of phase behavior as a function of small particle volume fraction, $\phi_{L,C}$ and $\phi_{U,C}$.

Chapter 5

Summary

5. Summary

This study reports a dramatic rheological and structural change, from fluid to gel, of a suspension of originally well-dispersed large particles, upon the addition of small particles, depending on the surface chemistry and concentration of small particles. The phase transition is sensitive to the surface chemistry and the amount of small particles. When the small particles have the opposite charge to the large particles, the phase changes from fluid to short bridging gel, and then to fluid again as the concentration of small particles increases. The short bridging gel is observed only in the narrow range of volume fraction, $10^{-4} < \phi_{small} < 10^{-3}$.

In contrast, when the small particles are attractive to each other, the phase changes from fluid to long bridging gel, and then to dense gel. The critical gel point of the small particles determines the boundary between the long bridging gel and dense gel. Repulsive small particles do not induce particle networks, remaining in a fluid state over the entire range of small particle volume fractions. A phase diagram of bimodal slurries was drawn based on the concentration and surface chemistry of nanoparticles.

A new type of colloidal gel was induced by a minute incremental addition of small particles, not described by the typical power - law scaling for

fractal clusters. This study suggests that this gel results from the formation of non-fractal networks of large particles which are bridged by small particle clusters in the range of $\phi_{L,C} < \phi_{small} < \phi_{U,C}$. It is expected that the discovery of this new regime of colloidal gels in the phase diagram advances our understanding of the complex behavior of size-asymmetric colloids.

Because the model fluid in this study is similar to the slurries used in industry with respect to the size ratio, the range of concentration, and the surface potential, It is expected that the slurries encountered in practice have analogous mechanical behavior and microstructure to this model fluid. This study consequently provides a guideline for the design of such complex fluids and understanding of their complex flow behavior. In addition, these methods and results confirm that the rheological properties can be tuned by using a small amount of inorganic nanoparticles as a substitute for organic binders, which often hinder the electrical performance of the final products.

Bibliography

1. Dominko, R., M. Gaberscek, J. Drofenik, M. Bele, S. Pejovnik and J. Jamnik, The role of carbon black distribution in cathodes for Li ion batteries. Journal of Power Sources, 2003. 119: p. 770-773.
2. Lee, G.-W., J. H. Ryu, W. Han, K. H. Ahn and S. M. Oh, Effect of slurry preparation process on electrochemical performances of LiCoO2 composite electrode. Journal of Power Sources, 2010. 195(18): p. 6049-6054.
3. Trappe, V. and D.A. Weitz, Scaling of the viscoelasticity of weakly attractive particles. Physical Review Letters, 2000. 85(2): p. 449.
4. Ueyama, R., K. Kuribayashi, and K. Koumoto, Fabrication and evaluation of Ni-MLCC used of new BaTiO3 resinate. Journal of the Ceramic Society of Japan, 2004. 112(1308): p. 458-461.
5. Kim, J., B. Kim, J. G. Lee, J. Cho and B. Park, Direct carbon-black coating on LiCoO2 cathode using surfactant for high-density Li-ion cell. Journal of Power Sources, 2005. 139(1-2): p. 289-294.
6. Ponrouch, A. and M.R. Palacín, On the impact of the slurry mixing procedure in the electrochemical performance of composite electrodes for Li-ion batteries: A case study for mesocarbon microbeads (MCMB) graphite and Co3O4. Journal of Power Sources, 2011. 196(22): p. 9682-9688.
7. Grunlan, J.C., W.W. Gerberich, and L.F. Francis, Electrical and mechanical behavior of carbon black-filled poly(vinyl acetate) latex-based composites. Polymer Engineering & Science, 2001. 41(11): p. 1947-1962.
8. Sun, J., W.W. Gerberich, and L.F. Francis, Electrical and optical properties of ceramic-polymer nanocomposite coatings. Journal of

Polymer Science Part B: Polymer Physics, 2003. 41(14): p. 1744-1761.
9. Asakura, S. and F. Oosawa, Interaction between particles suspended in solutions of macromolecules. Journal of Polymer Science, 1958. 33(126): p. 183-192.
10. Mao, Y., M.E. Cates, and H.N.W. Lekkerkerker, Depletion force in colloidal systems. Physica A: Statistical Mechanics and its Applications, 1995. 222(1–4): p. 10-24.
11. Imhof, A. and J.K.G. Dhont, Experimental phase diagram of a binary colloidal hard-sphere mixture with a large size ratio. Physical Review Letters, 1995. 75(8): p. 1662-1665.
12. Thierry, B., B. Peter, and F. Daan, Depletion effects in binary hard-sphere fluids. Journal of Physics: Condensed Matter, 1996. 8(50): p. 10799.
13. Sikorski, M., A.R. Sandy, and S. Narayanan, Depletion-induced structure and dynamics in bimodal colloidal suspensions. Physical Review Letters, 2011. 106(18): p. 188301.
14. Ashton, D.J., N. B. Wilding, R. Roth and R. Evans, Depletion potentials in highly size-asymmetric binary hard-sphere mixtures: Comparison of simulation results with theory. Physical Review E, 2011. 84(6): p. 061136.
15. Fernández-Barbero, A. and B. Vincent, Charge heteroaggregation between hard and soft particles. Physical Review E, 2000. 63(1): p. 011509.
16. Kim, A.Y. and J.C. Berg, Fractal Heteroaggregation of oppositely charged colloids. Journal of Colloid and Interface Science, 2000. 229(2): p. 607-614.
17. Puertas, A.M., A. Fernandez-Barbero, and F.J.D.L. Nieves, Charged colloidal heteroaggregation kinetics. The Journal of Chemical Physics, 2001. 114(1): p. 591-595.
18. Lin, W., M. Kobayashi, M. Skarba, C. Mu, P. Galletto and M.

Borkovec, Heteroaggregation in binary mixtures of oppositely charged colloidal particles. Langmuir, 2005. 22(3): p. 1038-1047.

19. López-López, J.M., A. Schmitt, A. Moncho-Jordá and R. Hidalgo-Álvarez, Electrostatic heteroaggregation regimes in colloidal suspensions. Advances in Colloid and Interface Science, 2009. 147-148: p. 186-204.
20. Tohver, V., A. Chan, O. Sakurada and J. A. Lewis, Nanoparticle engineering of complex fluid behavior. Langmuir, 2001. 17(26): p. 8414-8421.
21. Karanikas, S. and A.A. Louis, Dynamic colloidal stabilization by nanoparticle halos. Physical Review Letters, 2004. 93(24): p. 248303.
22. Scheer, E.N. and K.S. Schweizer, Haloing, flocculation, and bridging in colloid-nanoparticle suspensions. The Journal of Chemical Physics, 2008. 128(16): p. 164905-15.
23. Zhang, F., G. G. Long, P. R. Jemian, J. Ilavsky, V. T. Milam and J. A. Lewis, Quantitative measurement of nanoparticle halo formation around colloidal microspheres in binary mixtures. Langmuir, 2008. 24(13): p. 6504-6508.
24. Karimian, H. and A.A. Babaluo, Nanoparticle halos mechanism in stabilizing of colloidal suspensions: Polymeric binder and dispersant effects. Journal of Dispersion Science and Technology, 2011. 33(4): p. 457-464.
25. Bitsch, B., J. Dittmann, M. Schmitt, P. Scharfer, W. Schabel and N. Willenbacher, A novel slurry concept for the fabrication of lithium-ion battery electrodes with beneficial properties. Journal of Power Sources, 2014. 265(0): p. 81-90.
26. Wenzel, V., H. Nirschl, and D. Nötzel, Challenges in lithium-ion-battery slurry preparation and potential of modifying electrode structures by different mixing processes. Energy Technology, 2015. 3(7): p. 692-698.

27. Wu, S., X. Wei, X. Wang, H. Yang and S. Gao, Effect of Bi2O3 additive on the microstructure and dielectric properties of BaTiO3-based ceramics sintered at lower temperature. Journal of Materials Science & Technology, 2010. 26(5): p. 472-476.
28. Wang, Y. and C. Anderson, Formation of thin transparent conductive composite films from aqueous colloidal dispersions. Macromolecules, 1999. 32(19): p. 6172-6179.
29. Luo, H., C. M. Cardinal, L. E. Scriven and L. F. Francis, Ceramic nanoparticle/monodisperse latex coatings. Langmuir, 2008. 24(10): p. 5552-5561.
30. Brown, R.F.G., C. Carr, and M.E. Taylor, Effect of pigment volume concentration and latex particle size on pigment distribution. Progress in Organic Coatings, 1997. 30(3): p. 185-194.
31. Tiarks, F., T. Frechen, S. Kirsch, J. Leuninger, M. Melan, A. Pfau, F. Richter, B. Schuler and C.-L. Zhao, Effects on the pigment distribution in paint formulations. Macromolecular Symposia, 2002. 187(1): p. 739-752.
32. Dijkstra, M., R. van Roij, and R. Evans, Phase diagram of highly asymmetric binary hard-sphere mixtures. Physical Review E, 1999. 59(5): p. 5744-5771.
33. Cerbelaud, M., R. Ferrando, and A. Videcoq, Simulations of heteroaggregation in a suspension of alumina and silica particles: Effect of dilution. The Journal of Chemical Physics, 2010. 132(8): p. 084701-9.
34. Cerbelaud, M., A. Videcoq, P. Abelard, C. Pagnoux, F. Rossignol and R. Ferrando, Self-assembly of oppositely charged particles in dilute ceramic suspensions: predictive role of simulations. Soft Matter, 2010. 6(2): p. 370-382.
35. Cerbelaud, M., A. Videcoq, P. Abelard, C. Pagnoux, F. Rossignol and R. Ferrando, Heteroaggregation between Al2O3 submicrometer

particles and SiO2 nanoparticles: Experiment and simulation. Langmuir, 2008. 24(7): p. 3001-3008.

36. Hui, D., M. Nawaz, D. P. Morris, M. R. Edwards and B. R., Saunders Study of pH-triggered heteroaggregation and gel formation within mixed dispersions. Journal of Colloid and Interface Science, 2008. 324(1-2): p. 110-117.
37. Hui, D., D. Morris, M. R. Edwards and B. R. Saunders, A study of structure and temperature-triggered breakdown of particle gels prepared by pH-triggered heteroaggregation. Journal of Colloid and Interface Science, 2010. 342(2): p. 320-326.
38. Liu, J. and E. Luijten, Stabilization of colloidal suspensions by means of highly charged nanoparticles. Physical Review Letters, 2004. 93(24): p. 247802.
39. Tohver, V., A. Chan, O. Sakurada and J. A. Lewis, Nanoparticle halos: A new colloid stabilization mechanism. Proceedings of the National Academy of Sciences, 2001. 98(16): p. 8950-8954.
40. Sun, J., B. V. Velamakanni, W. W. Gerberich and L. F. Francis, Aqueous latex/ceramic nanoparticle dispersions: Colloidal stability and coating properties. Journal of Colloid and Interface Science, 2004. 280(2): p. 387-399.
41. Trappe, V., V. Prasad, L. Cipelletti, P. N. Segre and D. A. Weitz, Jamming phase diagram for attractive particles. Nature, 2001. 411(6839): p. 772-775.
42. Channell, G.M. and C.F. Zukoski, Shear and compressive rheology of aggregated alumina suspensions. Aiche Journal, 1997. 43(7): p. 1700-1708.
43. Buscall, R., P. D. A. Mills, J. W. Goodwin and D. W. Lawson, Scaling behaviour of the rheology of aggregate networks formed from colloidal particles. Journal of the Chemical Society, Faraday Transactions 1: Physical Chemistry in Condensed Phases, 1988.

84(12): p. 4249-4260.
44. Dinsmore, A.D., E. R. Weeks, V. Prasad, A. C. Levitt and D. A. Weitz, Three-dimensional confocal microscopy of colloids. Appl. Opt., 2001. 40(24): p. 4152-4159.
45. Chestnut, M.H., Confocal microscopy of colloids. Current Opinion in Colloid & Interface Science, 1997. 2(2): p. 158-161.
46. Dinsmore, A.D. and D.A. Weitz, Direct imaging of three-dimensional structure and topology of colloidal gels. Journal of Physics: Condensed Matter, 2002. 14(33): p. 7581.
47. Kang, M. and S. Lee, Rheological and electrical properties of polystyrene/multi-walled carbon nanotube nanocomposites prepared by latex technology. Korea-Australia Rheology Journal, 2012. 24(2): p. 97-103.
48. Eberle, A.P.R., N. J. Wagner, and R. Castañeda-Priego, Dynamical arrest transition in nanoparticle dispersions with short-range interactions. Physical Review Letters, 2011. 106(10): p. 105704.
49. Kim, J.M., J. Fang, A. P. R. Eberle, R. Castañeda-Priego and N. J. Wagner, Gel transition in adhesive hard-sphere colloidal dispersions: The role of gravitational effects. Physical Review Letters, 2013. 110(20): p. 208302.
50. Sorensen, C.M. and A. Chakrabarti, The sol to gel transition in irreversible particulate systems. Soft Matter, 2011. 7(6): p. 2284-2296.
51. Krieger, I.M., Rheology of monodisperse latices. Advances in Colloid and Interface Science, 1972. 3(2): p. 111-136.
52. Grant, M.C. and W.B. Russel, Volume-fraction dependence of elastic moduli and transition temperatures for colloidal silica gels. Physical Review E, 1993. 47(4): p. 2606.
53. Rueb, C.J. and C.F. Zukoski, Viscoelastic properties of colloidal gels. Journal of Rheology, 1997. 41(2): p. 197-218.
54. Shah, S.A., Y. L. Chen, K. S. Schweizer and C. F. Zukoski.,

Viscoelasticity and rheology of depletion flocculated gels and fluids. The Journal of Chemical Physics, 2003. 119(16): p. 8747-8760.

55. Laurati, M., G. Petekidis, N. Koumakis, F. Cardinaux, A. B. Schofield, J. M. Brader, M. Fuchs and S. U. Egelhaaf, Structure, dynamics, and rheology of colloid-polymer mixtures: From liquids to gels. The Journal of Chemical Physics, 2009. 130(13): p. 134907-14.
56. P.C. Hiemenz, Principles of colloid and surface chemistry. 1997, Dekker.
57. Sader, J.E., S.L. Carnie, and D.Y.C. Chan, Accurate analytic formulas for the double-layer interaction between spheres. Journal of Colloid and Interface Science, 1995. 171(1): p. 46-54.
58. Grant, M.C. and W.B. Russel, Volume-fraction dependence of elastic-moduli and transition-temperatures for colloidal silica-gels. Physical Review E, 1993. 47(4): p. 2606-2614.
59. Shih, W.-H., W. Y. Shih, S.-I. Kim, J. Liu and I. A. Aksay, Scaling behavior of the elastic properties of colloidal gels. Physical Review A, 1990. 42(8): p. 4772-4779.
60. Zackrisson, A.S., J.S. Pedersen, and J. Bergenholtz, A small-angle X-ray scattering study of aggregation and gelation of colloidal silica. Colloids and Surfaces A: Physicochemical and Engineering Aspects, 2008. 315(1-3): p. 23-30.
61. Poon, W.C.K., The physics of a model colloid-polymer mixture. Journal of Physics-Condensed Matter, 2002. 14(33): p. R859-R880.
62. Masschaele, K., J. Fransaer, and J. Vermant, Direct visualization of yielding in model two-dimensional colloidal gels subjected to shear flow. Journal of Rheology, 2009. 53(6): p. 1437-1460.
63. Nagarkar, S.P. and S.S. Velankar, Morphology and rheology of ternary fluid-fluid-solid systems. Soft Matter, 2012. 8(32): p. 8464-8477.

국문 초록

리튬이온배터리, MLCC 등의 제조공정에서는 제품의 품질을 향상시키기 위해 두 가지 이상의 입자로 코팅액을 제조한다. 이때 서로 다른 표면특성과 크기를 가진 입자는 현탁액 내에서 복잡하게 상호작용하기 때문에 일반적인 단일입자로 이루어진 현탁액의 거동과 다르게 예기치 않은 문제를 일으킬 수 있다. 따라서 재료의 분산 안정성과 유동특성의 파악이 품질 향상을 위해 필수적임에도 불구하고 이분산 현탁액과 관련된 기존의 연구들은 대부분 안정적으로 잘 분산된 나노입자를 다루고 있기 때문에 서로 다른 표면 특성과 크기를 가진 실제 산업재료에는 적용이 어렵다.

산업적으로 사용되는 실제 슬러리를 이루는 재료는 다양한 성분으로 인하여 구조 관찰이 용이하지 않고, 실험적으로 확보/구현하기 어려운 특성이 있다. 이러한 한계를 극복하기 위하여 본 연구에서는 산업재료를 대체할 수 있는 모델 슬러리를 고안하였다. 두 가지 크기의 구형입자를 (PS latex (500nm), Alumina coated silica (Ludox CL, 12nm)) 물에 분산시켜 서로 다른 표면과 크기를 가진 이분산 입자계를 제조하였다. 이 모델 슬러리를 이용하면 수용액상에서 pH를 변화시킴에 따라 다양한 표면상태를 지닌 이분산성 입자계를 모사할 수 있다. pH가 변함에 따라 큰 입자는 안정적으로 분산이 유지되지만 작은 입자의 표면은 안정하게 분산된 상태, 안정화되지 않은 상태, 큰 입자와 반대전하를 가지는 상태로 조절된다.

첫째로, pH 조절을 통한 작은 입자의 표면상태 변화가 이분산 현탁액의 유변물성에 미치는 영향을 연구하였다. 작은 입자의 표면상태와 첨가하는 농도에 따라 이분산 현탁액의 유변물성은 급격한 변화를 보였다. 큰 입자와 반대전하를 가지는 작은 입자가 첨가 되었을 때, 작은 입자의 농도가 $10^{-4} < \phi_{small} < 10^{-3}$ 인 범위에서 겔이 형성되었다. 이 범위에서 작은 입자가 큰 입자를 가교하여 겔을 이루는 구조를 관찰할 수 있었다. 안정화되지 않은 상태의 작은 입자가 첨가되었을 때, 작은 입자의 농도가 $\phi_{small} > 10^{-4}$ 인 범위에서 겔이 형성되었다. 작은 입자의 농도가 낮을 때에는 작은 입자가 큰 입자를 가교하여 겔을 형성하였고 작은 입자의 농도가 높아질 때에는 큰입자 주변에 밀집된 형태로 겔을 이루었다. 유변물성과 미세구조분석을 바탕으로, 작은 입자의 표면상태와 농도변화에 따른 이분산 현탁액의 상태를 도식화 하였다.

둘째로, 안정화되지 않은 작은 입자가 안정적으로 분산된 큰 입자로 이루어진 현탁액에 첨가될 때 겔화 거동을 분석하였다. 이때 형성되는 겔은 기존의 현탁액의 겔화 거동에서 벗어났다. 탄성계수가 입자농도에 대하여 두 가지 서로 다른 기울기를 가지는 거동을 보였다. 이러한 거동은 미세구조분석을 통해 작은 입자에 의해 형성된 큰 입자의 겔 구조가 fractal 구조에서 벗어나기 때문인 것으로 해석할 수 있었다.

본 연구를 통해 작은 입자를 소량 첨가하는 것이 이분산 현탁액의 구조와 거동을 결정한다는 것이 증명되었으며, 본 연구는 산업 전반에 적용되는 코팅액의 조성과 최종 물성의

관계를 이해하는 데 기여할 것으로 기대한다.

주요어: 이분산 현탁액, 크기 비대칭이 심한 입자, 스케일링 거동, 미세구조, 분산안정성